Response to referee 1 (report 1)

Main point 1)
In this latest revision, the authors have used a modification of the Miller-Tans (2003) approach to interpret the stable carbon isotopic composition of CO2 emissions from Nanjing and the greater Yangtze River Delta in China. In this modification, they use background CO2 mole fractions from Carbon Tracker for each data point, but they do not assume any δ13C value, which becomes embedded in the intercept of the correlation line. The slope gives the composition of the high-CO2 mixing end member, as for the original Miller-Tans approach. The authors compare results between this calculation and the Keeling Plot method in which neither the mole fraction nor the δ13C of the background are known but are assumed constant over the duration of the sampling period. It is unclear what their conclusion is from the comparison.

We now include the flux partitioning results obtained with the δ_S values from the Keeling method (Figures S3 and S4). A short paragraph is added to the Discussion Section:

"When the δ_S derived from the Keeling plot method was used for flux-partitioning, the results were much more erratic than shown in Figures 7 and 8 (Supplementary Figures S3 and S4). The uncertainty ranges of the monthly F_P and F_S were two to three times larger. The biological flux F_P for the YRD was out of range for 4 months, and did not display an obvious seasonal pattern (Supplementary Figure S3). These results support our choice of the modified Miller-Tans method as the preferred approach for inferring the overall $^{13}C/^{12}C$ ratio of the surface sources in this study."

Main point 2)
My major concern at this time is the standards used to calibrate the Picarro CO2 Isotopic Analyzer (G1101-i) for δ13C. Two standards with differing CO2 mole fractions are run, but the δ13C values are within uncertainty and are very different from the ambient measurements. Citing Bowling et al. (2005), the authors say "because the system measures the concentrations of the major and minor isotopologue independently, it is not critical that the calibration standard and the measurement target have matching isotope ratios." However, in the Bowling et al. paper the standard values are much closer to those being analyzed, and Bowling et al. (2005) say that it is "not critical that the calibration gases differed in isotope ratio", not that the calibration standards differ from the target air. The method used here, by Xu et al., assumes linearity over a very wide range. Perhaps the authors could borrow a couple of standard tanks to determine the calibration line for the instrument over this wide range of compositions and then use the temporal variations of their standards to adjust for drift of the instrument, as was done by Verhulst et al. (2016) for CO2 mole fraction.
Verhulst, K. R. et al., 2016, Carbon Dioxide and Methane Measurements from the Los Angeles Megacity Carbon Project: 1. Calibration, Urban Enhancements, and Uncertainty Estimates: Atmospheric Chemistry and Physics Discussions, p. 1–61, doi:10.5194/acp-2016-850-SC1.

This is a good idea, but unfortunately we could not implement this procedure because the detector of our analyzer failed at the end of the experiment.

It is very difficult to make calibration standards that vary over a wide range of the concentration and simultaneously have delta values that match the ambient target. Our experience with these optical instruments is that it is much more important to have standards that bracket concentration variations of the target than to have standards that have matching delta values. A good explanation can be found in Bowling et al. (2005). For example, in an experiment where we measured the 18O/16O ratio of water vapor, we used a calibration vapor stream whose delta value was 10 per mil higher than the delta value of the samples; We were able to achieve an accuracy of 0.1 per mil (Lee et al., J Atmos Oceanic Technol 22: 555-565). In Bowling et al. (2003), the calibration standards had much lower $\delta^{13}C$ values (-30 and -40 per mil) than the ambient delta, but because these standards bracketed the concentration range of the ambient measurement, their measurement accuracy was quite good (mean absolute difference less than 0.3 per mil between the in-situ measurement and flask sampling/mass-spectrometry).

In response, we have modified the text to:

"…These gases were balanced in air, and their concentration values bracketed the range of ambient concentration variability (Figure 3 below)."

"… The mismatch in the delta value between the calibration standard and the ambient air is common in applications of the IRIS technique [$^{13}C(CH_4)$, Röckmann et al. 2016; $^{18}O(H_2O)$, Lee et al. 2005; $^{13}C(CO_2)$, Bowling et al. 2003]. For example, Bowling et al. (2003) used calibration standards with delta values of -29.55 ‰ and -40.58 ‰ to calibrate their optical $^{13}C(CO_2)$ instrument. But because the system measures the concentrations of the major and the minor isotopologue independently, it is not critical that the calibration standards and the measurement target have matching isotope ratios, so long as the standards bracket concentration variability of the target (Bowling et al. 2005). Nevertheless, the overall accuracy of the measurement may be further improved by using calibration standards that bracket variations in both the concentration and the delta values of ambient air samples."

Specific comments:
(1)Line 65: "configuration" should be plural "configurations"
Edited.

(2)Line 83: Add "isotope ratio" before "mass-spectrometry" and change "MS" to "IRMS
Changed.

(3)Line 96: The Verdag et al. (2016) study is for simulated data only, not measurements.
Edited.

(4)Line 138: "method" should be plural "methods"
Edited.

(5)Line 167: Are you sure that these values are "before" normalization? They are probably on the VPDB scale. If not, please convert to VPDB.
These were actually expressed on the VPDB scale.

(6)Line 186: Add "the average" after "if".
Added.

(7)Line 188 and elsewhere: There are spurious "!" symbols. Please remove.
We could not find "!" anywhere in our original document. Perhaps it was inserted when the document was converted for viewing by the journal website.

(8)Lines 214-216: What results do you get if you force the correlations through zero?

If we forced zero intercept, the slope would be (-16.76 ± 0.49) ‰ for daytime and (-18.60 ± 0.41) ‰ for nighttime, which would be too high as the source 13C/12C ratio.

(9)Lines 230-232: Newman et al. (2016) gives all monthly Miller-Tans plots for 2011, forced through zero and no intercepts are obvious. No intercepts are required for the monthly plots over 8 years of data.

We were encouraged by the success that Newman et al. had with the Miller-Tans method. That is one of the reasons why we used this method for data interpretation. Perhaps the reason why Newman et al. were successful but we weren't was because the LA airshed has a well-defined air circulation pattern whose upwind (background) air can be directly measured.

We now cite this paper here:
"When applied to the urban airshed in Los Angles, Equation 1 does not require an intercept (Newman et al. 2016). But when applied to the data obtained at the monthly time scale in this study, the regression yielded a non-zero intercept (Supplementary Figure S2)."

Please also refer to our response to review 4, point 1.

(10)Line 239: Since you have Cb from CarbonTracker, you can calculate δb. Are the values reasonable? If not, then there is a problem with assumptions.

Please refer to our response to review 4, point 1.

(11)Line 243: At the end of the paragraph, insert a statement such as: "We call this a modified Miller-Tans analysis, which requires knowledge of CO2 mole fraction, but not δb.
Added. Thank you.

(12)Line 263: Replace "at" with "for".
Replaced.

(13)Line 291: Is FP the net biological flux? If so, it might be better to use "BIO", since "P" suggests photosynthesis, but this is photosynthesis + respiration.

This subscript was recommended by an earlier reviewer, to indicate plant biological flux but exclude human metabolism.

(14)Line 303: Insert "value for" before "δF" and "the" after "was".
Added.

(15)Line 307: "an U-shaped" should be "a U-shaped"
Edited.

(16)Line 322: "expression" should be plural "expressions"
Edited.

(17)Lines 322-330: How do the Monte Carlo analysis errors compare to an average explicit error propagation calculation?

The explicit error propagation calculation can be done if only one or two parameters have uncertainty but becomes very difficult if more parameters are involved. So we did not do this.

(18)Lines 343-344: Are these standard errors or standard deviations? Standard errors are probably more appropriate here.
Changed.

(19)Line 352: "Contrary" should be "In contrast".
Edited.

(20)Line 357: Insert "modified" before "Miller-Tans".
Added.

(21)Line 367: Delete ")" after "1.79".
Deleted.

(22)Line 383: Insert "combustion" after "fossil fuel".
Added.

(23)Line 384: Insert "manufacturing" after "pig iron".
Added.

(24)Lines 434-442: Comparison with Paris (Widory and Javoy, 2003), Los Angeles (Newman et al., 2016)?

On the recommendations by Reviewer 4, we have shortened this subsection. These papers are cited elsewhere in the paepr.

(25)Line 450: Add "of" after "difference".
Added.

(26)Line 454: Add "of" after "difference".
Added.

(27)Lines 508-510: What is the R2?
Added. (The R^2 is 0.88.)

(28)Line 533 "method" should be "methods"
Edited.

(29)Lines 536-538: Where does the value of 0.21 ‰ come from? Is this for all sources, both anthropogenic and biogenic? And is this difference significant?

The source 13C/12C ratio was determined with the modified Miller-Tans method from the atmospheric measurements, so it is for all sources.

This sentence has been improved as:
"The daytime measurement (Figure 6a, solid circles) revealed that the $^{13}C/^{12}C$ ratio of the all sources (anthropogenic and biological) was on average 0.21 ‰ higher than that obtained with the nighttime measurement (Figure 6b, solid circles), although the difference is not statistically significant (p = 0.38)."

(30)Line 539: "Table 2" should be "Table 3".
Corrected.

(31)Line 549: What is your interpretation of the bias between the two methods (Table S2)? What is your conclusion?

Please refer to our response to main point 1.

(32)Line 553: Replace "If" with "When".
Replaced.

(33)Line 557: The value of 0.21 ‰ seems much lower than the monthly differences observed

in Fig. 6b.
Thank you for catching this error. The difference is 1.21 ‰.

(34)Line 571: Insert "modified" before "Miller-Tans".
Inserted.

(35)Line 929: How does the background you used compare to the WLG data for CO2 mixing ratio?

This difference was provided in the Methods section (Section 2.2):

"The CarbonTracker mole ratio is on average 3.5 μmol mol^{-1} higher than that observed at WLG."

Response to referee 4 (report 2)

The manuscript reports about carbon isotope compositions on carbon dioxide (CO2) in the Yangtze River Delta of China with a high temporal resolution using a Cavity Ring-Down Spectroscopic method. They have analysed the data for daytime and nighttime behaviour independently and argued that these two datasets do represent different catchment area, i.e. the Yangtze River Delta area and the Nanjing municipality area, respectively. This is an adequate approach to retrieve information about two differently sized areas with only one measurement site. This approach was justified by corresponding back-trajectory analyses. The specificity of the assumption is however not further elaborated on. They have applied both the Miller-Tans as well as the Keeling approach to retrieve the source signatures for the isotope composition. Based on that very positive values in carbon isotopes, even in comparison with the background site at Mount Waliguan (WLG), they concluded that there must be a strong contribution from cement production, which is known to have a very high carbon isotopic composition.

I suggest revising the manuscript based on the suggestions given below (minor revision).

Main point 1)

Which equation to be used to derive the source signature?

They have analysed the day- and nighttime data using the Miller-Tans method to estimate the source signature for the carbon isotopic composition of CO2. Since they experience a significant offset when using the data from Mount Waliguan (WLG) as background values which should not be the case in this approach, they rearranged the Miller-Tans equation to allow for an offset (eq. 3 in their manuscript). This is of course allowed and will not change the interpretation of the results, yet it would allow the authors to estimate by how much the concentration or the carbon isotope composition has to be changed by assuming either constant Delta values of the background or concentration in order to resolve the problem of the observed offset applying eq. 1 in their manuscript. A quick calculation leads to either a mismatch of background CO2 values of more than 50 ppm (which is certainly unrealistic) or a change in the background Delta value of about +1 permil. It might be worthwhile to discuss these numbers. It might give us additional information of how extended the influence of cement production signals is in this area investigated.

This is an excellent point. The δ_b value backed out from the intercepts shown in Figures 4 and 5 is -7.6 ‰, which is higher than expected. In response to this comment, we have added a short paragraph in the Discussion Section:

"One open question with regard to the modified Miller-Tans method is what constitutes the true background air for the YRD. In this study, the background was assumed to be the tropospheric air above the YRD. The background delta value (δ_b) backed out from the intercepts shown in Figures 4 and 5 is -7.6 ‰, which is higher than expected, suggesting that the true background concentration C_b may be higher than the tropospheric value. One noteworthy feature about Equation 3 is that its slope parameter is not sensitive to C_b, but its intercept parameter is. By increasing C_b by 15 μmol mol^{-1}, the slope of the regression in

Figure 5 would remain unchanged, but the δ_b backed out from the new intercept value would be become more reasonable (-8.23 ‰). In Newman et al. (2016), the background air was measured at a coastal location upwind of the Los Angles airshed. It is recommended that a similar strategy should be used in future experiments, where simultaneous measurement is made at the coast of East China Sea and only data collected in easterly winds are used for the Miller-Tans analysis."

Main point 2)
Precision of the instrument
The manufacturer typical 5 minute precision of 0.3 per mil is actually the same as for your own measurements precision of 0.05 per mil per hour. It is simply a statistical improvement. Please change accordingly.

We have added this sentence here:
"These improvements were simply statistical, due to the increase in the number of samples being used for averaging."

Main point 3)
The filtering procedure
The criteria for the filtering procedure are neither well motivated nor justified. Why these limits?

We have added some details here:

"Additionally, data were removed if the average hourly CO_2 mole fraction was lower than 390 μmol mol^{-1} (or 30 μmol mol^{-1} lower than the midafternoon value in the summer; Figure 3 below) or $\delta^{13}C$ were out of the range between -15 ‰ and -5.5 ‰ (or about 3 standard deviations from the mean); A total of 217 hourly values were removed by these outlier criteria."

Main point 4)
The standards used are inadequate
As already pointed out by other reviewers during the publishing procedure. The standard are inadequate for this analyses. They must be in the range of the outside air variations that is measured. Yet, they cannot resolve this problem for the past, but they can take action now and replace these standards. Such a statement should be placed in this publication.

We have added a sentence here:
"Nevertheless, the overall accuracy of the measurement may be further improved by using calibration standards that bracket variations in both the concentration and the delta values of ambient air samples."

Please also refer to our response to Reviewer 1, main point 2.

Main point 5)
Water correction
The water correction is quite significant and I am puzzled that the manufacturer does not apply such a correction. Am I right, that you have to do this correction. But I hope that the water vapor measurement is done by the same system or do you need to use a separate one? There is also not mentioned for how long you have been measuring the standard air at the different water vapor levels during the water correction calibration. This should be added to make sure that there are no transient signals involved. Furthermore, the precision of the water correction is not very high (see Figure 1). I guess this can be significantly improved and should be made with additional experiments for future publications.

The water vapor measurement was done by the same system. The precision here is worse than that reported for hourly means because it was based on 1-min averages. Each measurement lasted 30 min.

These details are now included in the revision:

"…Measurement at each humidity level lasted 30 min, with the first 5-min excluded from the analysis … where H2O is water vapor mole fraction was measured by the same isotope analyzer."

"Figure 1 caption: … Error bars are ± one standard deviation of 1-min averages."

Main point 6)
Flux calculations
I wonder whether the flux calculations are indeed very helpful for the main conclusion that the cement production has a major influence on carbon isotopic composition in this area. The estimations are not further checked by for instance radon measurements.

Thank you for your comments. We included the partition result in part to support our interpretation about the role of cement production. One conclusion is that biological fluxes were small in the YRD. If the biological fluxes were much larger, we might not be able to detect the cement influence.

Main point 7)
The introductions as well as the discussion part 4.1 can significantly be condensed.

We have shortened Section 4.1 by about 50 % and the Introduction section by about 15 %.

Specific comments:
(1)Eq 1: It might be worthwhile to use a time-dependent formulation (i.e. all variables are time dependent.

We have added a short sentence below Equation 1:
"All the variables are time dependent."

(2)Line 159: Figure S1).
Edited.

(3)Line 162: NOAA-ESRL
Edited.

(4)Line 204: The percent unit is missing after 2.03
Added.

(5)Line 310: …of the four source ….
Edited.

(6)Line 337f: CO2 mole fraction during the whole experiment period (March 2013 to august 2015) was ….
Edited.

(7)Line 346: compare to seasonality at Nanjing.
Edited.

(8)Line 437: higher instead of greater
This sentence has been deleted

(9)Line 490: This delta 13C …
Edited.

(10)Line 529: digestion instead of respiration
Edited.

(11)Fig. 1: It would be helpful to make a comparison to Rella 2011 values.

We have added a sentence to the main text:
"This humidity effect is not negligible, but is an order of magnitude smaller than that reported by Rella (2011)."

Interpreting the $^{13}C/^{12}C$ ratio of carbon dioxide in an urban airshed in the Yangtze River Delta, China

Jiaping Xu[1], Xuhui Lee[1,2*], Wei Xiao[1], Chang Cao[1], Shoudong Liu[1], Xuefa Wen[3], Jingzheng Xu[1], Zhen Zhang[1], Jiayu Zhao[1]

[1]Yale-NUIST Center on Atmospheric Environment, Nanjing University of Information Science & Technology, Nanjing, China

[2]School of Forestry and Environmental Studies, Yale University, New Haven, Connecticut, USA

[3]Key Laboratory of Ecosystem Network Observation and Modeling, Institute of Geographic Sciences and Natural Resources Research, Chinese Academy of Sciences, Beijing, China

* Corresponding author
Dr. Xuhui Lee
Sara Shallenberger Brown Professor
School of Forestry and Environmental Studies, Yale University,
21 Sachem Street, New Haven, Connecticut 06510, USA
Phone: (203)432-6271; Fax: (203)432-5023
E-mail: xuhui.lee@yale.edu

Abstract: Observations of atmospheric CO_2 mole fraction and the $^{13}C/^{12}C$ ratio (expressed as $\delta^{13}C$) in urban airsheds provide constraints on the roles of anthropogenic and natural sources and sinks in local and regional carbon cycles. In this study, we report observations of these quantities in Nanjing at hourly intervals from March 2013 to August 2015 using a laser-based optical instrument. Nanjing is the second largest city located in the highly industrialized Yangtze River Delta (YRD), Eastern China. The mean CO_2 mole fraction and $\delta^{13}C$ were (439.7 ± 7.5) μmol mol^{-1} and (-8.48 ± 0.56) ‰ over this observational period. The peak monthly mean $\delta^{13}C$ (-7.44 ‰, July 2013) was 0.74 ‰ higher than that observed at Mount Waliguan, a WMO baseline site on the Tibetan Plateau and upwind of the YRD region. The highly ^{13}C-enriched signal was partly attributed to the influence of cement production in the region. By applying the Miller-Tans method to nighttime and daytime observations to represent signals from the city of Nanjing and the YRD, respectively, we showed that the $^{13}C/^{12}C$ ratio of CO_2 sources in the Nanjing Municipality was (0.21 ± 0.53) ‰ lower than that in the YRD. Flux partitioning calculations revealed that natural ecosystems in the YRD were a negligibly small source of atmospheric CO_2.

Keywords: urban areas; CO_2 flux; Industrial process; Carbon isotope; In-situ observation

1 Introduction

Atmospheric CO_2 sources and sinks in urban areas consist mainly of plant uptake and release and fossil fuel combustion. These contributors have unique $^{13}C/^{12}C$ ratios. City clusters are human-dominated systems with high carbon emission intensity, contributing over 70% of the total anthropogenic CO_2 to the atmosphere (Satterthwaite 2008). Previous urban isotopic studies emphasize carbon emissions from fossil combustion (Zondervan and Meijer 1996, Pataki et al. 2003, Zimnoch et al. 2004, Affek and Eiler 2006, Newman et al. 2008). Relatively little attention is given to the $\delta^{13}C$ of carbon dioxide released by cement production, which is much higher than that of fossil fuel origin (Andres et al. 1994). Likewise, the CO_2 emitted from burning of minerals in non-energy consumption industrial processes, such as iron and steel production, has higher $\delta^{13}C$ than that of fossil fuel (Table 2, Widory 2006). In China, cement production and industrial processes contribute 13 % of the total anthropogenic CO_2 emission (Mu et al. 2013). Many of these industrial activities occur in or near urban areas. So far, little is known about their roles in the atmospheric carbon stable isotope budget.

One scientific motivation for quantifying the $\delta^{13}C$ of atmospheric CO_2 is that it provides constraints that allow partitioning of the net surface flux into component fluxes (Farquhar and Lloyd 1993, Yakir and Sternberg 2000, Pataki et al. 2003). The ^{13}C-based partitioning method has been used primarily for vegetation ecosystems, such as forests (Lloyd et al. 1996, Lloyd et al. 2001, Ometto, et al. 2006, Zobitz et al. 2008), grasses (Ometto et al. 2002, Pataki et al. 2003), and crops (Leavitt et al. 1995, Griffis et al. 2005). The approach has also been used in a limited number of urban studies (Pataki et al. 2003, Zimnoch et al. 2004, Newman et al.

2008, Jasek et al. 2014). Compared with vegetation ecosystems, urban ecosystems have more complex CO_2 source configurations. We must consider both natural sources (plants and soils) and anthropogenic sources (fossil combustion and non-energy industrial processes) and the fact that the degree of mixing of urban air with the free troposphere and the air outside the urban boundary varies diurnally and seasonally. Anthropogenic emissions are hard to quantify because they depend on multiple factors including city size, population density, fossil mix, and climate.

One of the first measurements of the carbon isotope ratio of CO_2 in an urban atmosphere was made by Friedman and Irsa (1967). Since then, ~~a few~~ more experiments have been conducted in urban environments~~. The data collected have been used to partition CO_2 contributors (~~ (Ehleringer et al. 2002, Koerner and Klopatek 2002, Takahashi et al. 2002, Clark-Thorne and Yapp 2003, Lichtfouse et al. 2003, Widory and Javoy 2003, ~~), to quantify diel variations in the CO_2 mole fraction and $\delta^{13}C$ in urban air (~~Zimnoch et al. 2004, Bush et al. 2007, Guha and Ghosh 2010~~,) and across urban to rural gradients (Lichtfouse et al. 2003, Pataki et al. 2007), and variations among different land uses in urban areas (Clark-Thorne and Yapp 2003, Widory and Javoy 2003). The isotopic data reveal insights into energy consumption patterns (Widory and Javoy 2003, Bush et al. 2007), impacts of meteorology including temperature (Clark-Thorne and Yapp 2003, Zimnoch et al. 2004), atmospheric stability (Pataki et al. 2005) and wind (Clark-Thorne and Yapp 2003) on urban carbon cycling, and the role of vegetation phenology (Ehleringer et al. 2002, Takahashi et al. 2002,~~ Wang and Pataki 2012). The analytical technique employed in these studies is mainly based on isotope-ratio mass-spectrometry (IRMS). ~~Because sample collection, preparation and~~

~~analysis are labor intensive, the majority of these studies are limited to short campaigns (less than 60 days).~~

In recent years, the development of isotope ratio infrared spectroscopy (IRIS) and on-line calibration technology provides a new solution for long-term in-situ observation of the CO_2 mole fraction and $\delta^{13}C$ at high frequencies (1 Hz to 1 hour; Pataki et al. 2006, Griffis. 2013, Gorski et al. 2015). ~~Compared with the MS method, IRIS can capture diel or even shorter temporal variations with relatively high accuracy, enabling us to understand how anthropogenic emissions change atmospheric CO_2 at highly resolved temporal and spatial scales.~~ However~~Nevertheless~~, application of the IRIS technology in urban monitoring is still limited in terms of cities covered and measurement duration ~~: less than 35 days in~~(~~-~~McManus et al. ~~(~~2002~~)~~, Pataki et al. 2006, ~~and~~ Wada et al. ~~(~~2011, ~~) and 3 seasons in~~ Moore and Jacobson (2015). Only a few published studies have presented data that span one full annual cycle (e.g., Pang et al. 2016~~; Vardag et al. 2016~~).

Simultaneous measurement of atmospheric CO_2 concentration and $\delta^{13}C$ is used to determine the overall $^{13}C/^{12}C$ ratio of local surface sources δ_S. The majority of published urban studies to date have deployed the Keeling plot method (Keeling 1958, Keeling 1961) for the determination of δ_S. In this approach, a linear relationship is established between $\delta^{13}C$ and the reciprocal of the CO_2 mole fraction from the observed time series, and the intercept of the linear regression is taken as the isotopic ratio of the local CO_2 emissions. The method assumes that the isotopic ratio of the sources is invariant with time. It also assumes that changes in the CO_2 mole fraction and in $\delta^{13}C$ are attributed only to the surface sources and are unaffected by regional carbon sources (Pataki et al. 2003). However, these assumptions

Formatted: Indent: First line: 2 ch

do not strictly hold in an urban environment because the intensity of traffic emissions varies strongly through the diel cycle (McDonald et al. 2014), and therefore the composition of the surface source varies, and its $^{13}C/^{12}C$ ratio cannot be assumed constant. In addition, because of strong atmospheric mixing in the daytime convective boundary layer, the background air in the upper troposphere can be easily entrained to the surface layer, mixing the CO_2 that originates from regional sources with that emitted locally in the urban airshed.

Miller and Tans (2003) propose that δ_S be determined as the slope of the linear relationship

$$\delta_a C_a - \delta_b C_b = \delta_S (C_a - C_b) \quad (1)$$

where C_a is CO_2 mole fraction in urban air, C_b is CO_2 mole fraction at a background site, δ_a is the $\delta^{13}C$ value of C_a, and δ_b is the $\delta^{13}C$ value of C_b. All the variables are time dependent. Because this approach takes into account the fact the background atmosphere varies, it may be more suitable than the Keeling method for inferring δ_S from the observations made in the urban area with complex emission sources. The method has been applied to local and regional carbon budget studies in nonurban settings (Miller et al. 2003) and in an urban environment by Newman et al. (2016). Here we extend the method to continuous measurements in an urban environment.

In this study, we report the results of long-term (30 months) continuous measurement of atmospheric CO_2 mole fraction and $\delta^{13}C$ at a suburban site in Nanjing using an IRIS instrument. Nanjing is the second largest city in the Yangtze River Delta (YRD), Eastern China, with a built-up area of 753 km^2 and a population of 8.2 million. Geographically, the YRD includes the provinces of Jiangsu, Zhejiang and Anhui and the Shanghai municipality

(29.04° to 33.41° N, 118.33° to 122.95° E) with a population of 190 million. The YRD is influenced by subtropical moist monsoon climate. The mean annual temperature is about 15 ^{o}C and the annual precipitation is between 1000 mm and 1800 mm. The vegetation types are all C3 species. The YRD is the most industrialized region in China and had a higher urban land fraction of 10.8 % as of 2014 than the global mean (2.4 %, Akbari et al. 2009). In 2014, more than 220 large cement production factories (daily output exceeding 1000 tons) were located in the YRD (China Cement, 2016), contributing about 20 % of the national cement output.

The objectives of this study are (1) to characterize the atmospheric δ^{13}C diel, seasonal and annual variations in this urban environment, in a region where such measurement is nonexistent, (2) to investigate the influence of cement production on atmospheric δ^{13}C, (3) to evaluate the performance of the Keeling plot and the Miller-Tans methods for determining δ_S, and (4) to explore the utility of the isotopic constraints for inferring the net surface flux and the plant CO_2 flux in Nanjing and in the YRD.

2 Methods

2.1 Atmospheric observation

An IRIS analyzer (model G1101-i, Picarro Inc., Sunnyvale, CA) was used to measure atmospheric CO_2 mole fraction and $^{13}C/^{12}C$ ratio (δ^{13}C) continuously from February 2013 to August 2015. The analyzer was housed on the 9th floor of our laboratory building on the campus of Nanjing University of Information, Science and Technology (NUIST, 32°12' N, 118°43' E), in the northern suburb of Nanjing, at a linear distance of 20 km to the city center.

The instrument inlet was at a height of 34 m above the ground. There was no large industrial CO_2 source in the 3 km radius except for a commuting road located about 300 m east of the observation site. The nearest industrial complex, the Nanjing Iron & Steel Group Co. Ltd. and the Nanjing Chemical Industry Group, was located about 5 km to the south of the site.

The measurement was made at 0.3 Hz and at an air flow rate of 30 mL min^{-1} at standard temperature and pressure. One three-way solenoid valve was combined with two two-way solenoid valves, so the analyzer could be switched for atmospheric sampling and for sampling of two standard gases. Calibration was carried out every 3 h by sampling each standard gas for 5 minutes following the procedure of Bowling et al. (2003) and Wen et al. (2013). [~~(~~To avoid transient effects, only the data collected in the last 2 minutes of the 5-min calibration periods was used (~~;~~ Supplementary Figure S1).]~~)~~ Table 1 lists the concentrations and their isotopic ratios of the standard gases used in this study. These gases were balanced in air, and their concentration values bracketed the range of ambient concentration variability (Figure 3 below). ~~–~~Their CO_2 mole fractions were measured with a gas analyzer (model (model G1301, Picarro) and calibrated against three primary standards obtained from NOAA-ESRL which were traceable to the WMO 2007 scale reported by the Central Calibration Laboratory of the World Meteorological Organization, and their $\delta^{13}C$ values were measured with a mass spectrometer (MAT-253, Finnigan) using IAEA reference materials IAEA-CO-8 (-5.76 ‰ ~~%~~ VPDB) and IAEA-CO-9 (-47.32 ‰ VPDB). The mass spectrometer measurements of these reference materials were (-5.81 ± 0.04) ‰ and (-46.64 ± 0.08) ‰ ~~before normalization to the VPDB scale~~. The ambient measurement was averaged to hourly

intervals. The isotopic ratio was expressed in the delta notation ($\delta^{13}C$) in reference to the VPDB scale.

The typical 5-min measurement precision is 0.3 ‰ for $\delta^{13}C$ and 0.05 μmol mol^{-1} for CO_2 mole fraction according to the instrument manufacturer. Our own Allan variance analysis revealed a precision of 0.05 ‰ for $\delta^{13}C$ and 0.07 μmol mol^{-1} for CO_2 mole fraction at the hourly averaging interval. These improvements were simply statistical, due to the increase in the number of samples being used for averaging. The precision of the ambient measurement was lower than this due to errors propagated through the calibration procedure. According to a laboratory test on an analyzer of the same model and using the same calibration procedure as ours, the hourly $\delta^{13}C$ precision is about 0.4 ‰ (Wen et al., 2013).

The calibration gases had much lower $\delta^{13}C$ than the ambient delta values. The mismatch in the delta value between the calibration standard and the ambient air is common in applications of the IRIS technique [$^{13}C(CH_4)$, Röckmann et al. 2016; $^{18}O(H_2O)$, Lee et al. 2005; $^{13}C(CO_2)$, Bowling et al. 2003]. For example, Bowling et al. (2003) used calibration standards with delta values of -29.55 ‰ and -40.58 ‰ to calibrate their optical $^{13}C(CO_2)$ instrument. But because the system measures the concentrations of the major and the minor isotopologue independently, it is not critical that the calibration standards and the measurement target have matching isotope ratios, so long as the standards bracket concentration variability of the target (Bowling et al. 2005). Nevertheless, the overall accuracy of the measurement may be further improved by using calibration standards that bracket variations in both the concentration and the delta values of ambient air samples.

Formatted: Font color: Text 1

We did not adopt the strict filtering technique used for background sites (Thoning et al. 1989) because of high natural variations in urban airsheds. We removed the first 3 min of the data after switching to the ambient sampling mode from the calibration mode. Additionally, data were removed if the average hourly CO_2 mole fraction was lower than 390 μmol mol^{-1} (or 30 μmol mol^{-1} lower than the midafternoon value in the summer; Figure 3 below) or $\delta^{13}C$ were out of the range between -15 ‰ and -5.5 ‰ (or about 3 standard deviations from the mean); A total of 217 hourly values were removed by these outlier criteria.

The $\delta^{13}C$ value measured by the analyzer in high humidity conditions is biased high due to spectral broadening and direct spectral interference (Rella 2011). To correct for the humidity interference, we carried out two tests using a dew-point generator (model 610, LI-COR, Inc., Lincoln, NE). A CO_2 standard gas (secondary standard gas, 439 μmol mol^{-1} in test one and 488 μmol mol^{-1} in test two, balanced by dry air) was fed into the dew-point generator. The outlet of the dew-point generator was connected with a 3-way union with one end linked to the inlet of the analyzer and the other open to the room. The humidity level of the air coming out of the dew point generator was regulated at eight levels in a dew-point temperature range of 1 to 30 °C, giving a water vapor mole fraction ranging from 0.66 % to 4.26 % (0.66 to 4.26 cmol mol^{-1}). Measurement at each humidity level lasted 30 min, with the first 5 min excluded from the analysis. Because the $^{13}C/^{12}C$ ratio of the standard gas was constant, any observed variations were caused by the humidity artifact. We found that no correction was needed for our analyzer if the water vapor mole fraction was below 2.03 %. Above this humidity level, the measurement was biased high by 0.46 ‰ for every 1 cmol mol^{-1} increase in the water vapor mole fraction (Figure 1). This humidity effect is not

negligible, but is an order of magnitude smaller than that reported by Rella (2011). The two tests, taken eight months apart, yielded essentially the same result. The correction equation is

$$\delta^{13}C = \delta^{13}C_{true} \qquad H_2O \leq 2.03\ \% \qquad (2a)$$

$$\delta^{13}C = \delta^{13}C_{true} + 0.46\ ‰\ (H_2O\ \% - 2.03\ \%) \qquad H_2O > 2.03\ \% \qquad (2b)$$

where H_2O is water vapor mole fraction and was measured by the same isotope analyzer, $\delta^{13}C$ is the measured isotope delta value (after the two-point calibration), and $\delta^{13}C_{true}$ is the true isotope delta value. The ambient vapor mole fraction varied from 0.16 to 3.64 % during the measurement period. About 35 % of the observations exceeded the threshold mole fraction of 2.03 % and required correction. The largest hourly correction was 0.74 ‰. In the following, all the data have been corrected for the humidity interference.

2.2 The $^{13}C/^{12}C$ ratio of surface sources (δ_S)

We applied the Miller-Tans method to estimate the $^{13}C/^{12}C$ ratio of the surface source (δ_S). Strictly, Equation 1 does not allow a non-zero intercept. When applied to the urban airshed in Los Angles, Equation 1 does not require an intercept (Newman et al. 2016). But when applied to the data obtained at the monthly time scale in this study, the regression yielded a non-zero intercept (Supplementary Figure S2). To determine if a shorter time scale would improve the result, we applied the 5-h moving window technique described by Vardag et al. (2016) to the observations made in January and July 2014. Only 4 % of the data, all obtained at nighttime, satisfies their data screening criteria. The mean regression equation of this subset is y = (-26.41 ±4.03) x + (428.84 ± 211.12) for January and y = (-25.64 ±6.39) x + (687.83 ± 264.67) for July, where x is (C_a - C_b) and y is ($\delta_a C_a$ - $\delta_b C_b$). In these analyses, the

238 background CO_2 mole fraction and the isotope ratio were those observed at Mount Waliguan
239 (WLG, 36°17' N, 100°54' E, 3816 m above the mean sea level;
240 https://www.esrl.noaa.gov/gmd/dv/data/index.php) located at the northeastern edge of the
241 Tibetan Plateau (Zhou et al., 2005), the closest upwind WMO background station for
242 Nanjing. Use of other WMO baseline sites as the background gave essentially the same
243 results.

244 The selection of a background site is a critical issue when applying the Miller-Tans
245 method (Ballantyne et al., 2011 & 2010). That the Miller-Tans intercept does not go to zero
246 suggests that the baseline site WLG may not be a suitable background for this highly
247 urbanized region. We tested the Miller-Tans method with other isotope data published for
248 urban areas, and found that the intercept was nonzero for most of the urban datasets
249 (Supplementary Figure S3 and Table S1).

250 In the following, we used the tropospheric CO_2 mole ratio calculated by CarbonTracker
251 over the YRD region (altitude 3330 m; https://www.esrl.noaa.gov/gmd/dv/data/index.php) as
252 the background concentration (C_b). The CarbonTracker mole ratio is on average 3.5 μmol
253 mol^{-1} higher than that observed at WLG. To overcome the problem that CarbonTracker does
254 not calculate tropospheric $\delta^{13}C$, we rearranged Equation 1 to a form that allows an intercept
255 but without the need for a known background $\delta^{13}C$, as

256 $$\delta_a C_a = \delta_S (C_a - C_b) + \delta_b C_b \quad (3)$$

257 The $^{13}C/^{12}C$ ratio of the surface source was taken as the slope of the linear regression of $\delta_a C_a$
258 against $(C_a - C_b)$. A key difference between Equation 3 here and Equation 5 of Miller and Tans
259 (2003) is that the δ_S appears only in the slope parameter in Equation 3 but in both the slope

and the intercept parameter in Miller and Tans' Equation 5. This modified Miller-Tans analysis requires knowledge of background CO_2 mole fraction but not δ_b.

The Miller-Tans analysis was performed over monthly intervals, using the data collected in daytime hours (10:00 to 16:00 local time) to represent YRD and data collected during nighttime hours (22:00-6:00 local time) to represent Nanjing. Morning and evening transitional periods were omitted to avoid the confounding effects of sign change of the biological CO_2 flux and sudden changes in the atmospheric stability regime.

We interpreted the daytime results to represent the influence of surface sources in the YRD region and the nighttime results to represent the influence of surface sources in the Nanjing municipality. The vigorous turbulent exchange in the daytime boundary layer diminishes the role of local sources in the measured concentration and isotopic ratio. In other words, the daytime measurement has a much larger source footprint than the size of the urban land itself or the footprint of the nighttime measurement. In contrast, the buildup of CO_2 at night is primarily the result of sources in the city (Shen et al. 2014), so we considered the δ_S determined from the nighttime observations to represent the signal of the sources located in the city. Admittedly, this interpretation of daytime versus nighttime source areas is a simplification because the actual source area also depends on thermal stratification and boundary layer wind. Nevertheless, it is supported by a trajectory analysis and by an analysis of the atmospheric methane to CO_2 emissions ratio (Shen et al. 2014).

For the purpose of comparing with the Miller-Tans results, we also estimated the source $^{13}C/^{12}C$ ratio using the Keeling mixing line method. According to Wehr and Saleska (2017), for~~at~~ the measurement uncertainties of our instrument system, the ordinary least squares

Formatted: Font: Not Italic

Formatted: Font: Not Italic

Formatted: Subscript

Formatted: Font: Not Italic

Formatted: Font: Not Italic, Subscript

282 procedure has much lower bias errors of parameter estimation than the geometric mean
283 regression. In the following, the results of both the Miller-Tans method and the Keeling
284 mixing line method were based on the ordinary least squares regression.
285
286 **2.3 Inventory of anthropogenic sources**
287 We calculated the anthropogenic CO_2 fluxes from energy consumption and industrial process
288 following the SCOPE 1 procedure issued by the International Council for Local
289 Environmental Initiatives (ICLEI, 2008). The procedure considers only emissions from
290 sources that lie within the geographic boundary of investigation. The energy consumption
291 source consists of direct emissions from the three main energy consumption sectors (industry,
292 transport, and household). We ignored the commerce sector here because the main energy
293 consumption in this sector in Nanjing and in the YRD was electric power generated by coal
294 and coal consumption which was already considered in SCOPE 1. The amounts of CO_2
295 emission were estimated with the IPCC methodology adopting the emission factors for each
296 fossil fuel type recommended by IPCC. The calculations were done separately for the YRD
297 region and for the Nanjing municipality. Because no statistical data were available for energy
298 consumption in the transport sector in Nanjing, the CO_2 emission from the transport sector
299 was deduced according to vehicle number, average annual driving distance and coefficients
300 of fuel economy (Bi et al. 2011). We obtained the data on energy consumption from official
301 sources (CESY 2013, CSY 2013, NSY, 2013).

The non-energy industrial processes included cement, raw iron, crude steel, and ammonia synthesis processes. In the YRD, the data were available at monthly intervals. For the city of Nanjing, only annual statistics were available.

2.4 Partitioning the net surface flux

We partitioned the surface CO_2 flux (F_S) into three component fluxes according to the following mass conservation equations

$$F_S = F_F + F_C + F_P \quad (4)$$

$$\delta_S F_S = \delta_F F_F + \delta_C F_C + \delta_P F_P \quad (5)$$

where F_F is the flux from fossil fuel combustion and industrial emission except cement production (termed "fossil plus"), F_C is the flux due to cement production, F_P is the biological flux, and δ_F, δ_C, and δ_P are the $\delta^{13}C$ value of F_F, F_C and F_P, respectively. These CO_2 mass fluxes are obtained by dividing the total emission by the surface area within the geographic boundary of Nanjing or the YRD, having dimensions of mg m^{-2} s^{-1}. We separated the cement source from other non-energy consumption industrial processes because its $^{13}C/^{12}C$ ratio is much higher. In these equations, the monthly net surface flux (F_S) and the biological flux (F_P) are unknowns to be solved for, and all other terms are either provided by the atmospheric measurement or by the inventory calculation. The partitioning analysis was done for both Nanjing and the YRD using the nighttime and daytime observations, respectively.

The value for δ_F was the weighted average of the isotope ratio of individual fuel types and industrial processes (Table 2). The delta value of CO_2 from cement production is provided by Anders (1994). We adopt a value of (-28.2 ‰) for δ_P for the YRD and Nanjing,

on account of a linear relationship between δ_P and tree age (Fessenden and Ehleringer 2002), a typical tree age in this region (40 years) and a~~n~~ U-shaped relationship between δ_P and annual precipitation (Pataki et al. 2007). Our δ_P is more negative than that reported for a boreal forest (-26.2 ‰; Pataki et al. 2007) but is in closer agreement with the value reported for a Ginkgo tree in Nanjing (-29.3 ‰; Sun et al. 2003). A summary of the isotopic ratios of the four~~three~~ source categories is given in Table 3.

Uncertainties in the delta values of the different fuel types and industrial processes were based on the data found in the references listed in Table 2. The uncertainty in δ_P was assumed to be ± 1.00 ‰ (Verdag et al. 2016). The mass flux terms F_F and F_C were assumed to have a 10% uncertainty, which is typical of fossil fuel consumption data (Vardag et al. 2016).

To partition the nighttime flux for Nanjing, we assumed that the nighttime F_F was 20 % of the daily value. The parameter 20 % was determined by the diel variation of the CO_2 flux observed with an eddy covariance system in Nanjing (Bai 2011) and in several other cities (Coutts et al. 2007, Song and Wang. 2011, Liu et al. 2012). At night, most of the factories in the city were closed and the traffic flow was reduced to about 80 % of the daytime volume (Yang et al. 2011).

The partitioning equations are explicit expressions of the mass balance principle. But uncertainties in the isotope delta end members and the anthropogenic fluxes can propagate through these equations, causing uncertainties in the estimation of F_S and F_P. Here we used a Monte Carlo analysis to quantify the error propagation. The same analysis has been applied to the partitioning of lake water budgets from isotope end members (Jasechko et al. 2014). The procedure employed a Gaussian distribution for errors in the input variables and an

ensemble of 10,000 realizations for each month. Errors in F_S and F_P were computed as one standard deviation of these realizations after excluding the top and bottom 50 extreme ensemble members.

3. Results

3.1. Temporal variations in the CO_2 mole fraction and $\delta^{13}C$

The monthly CO_2 mole fraction during the summer was slightly lower than in the other seasons (Figure 2). The mean mole fraction was 446.7 μmol mol^{-1} and 431.1 μmol mol^{-1} for January and July, respectively, giving a seasonal amplitude of 15.6 μmol mol^{-1}. The mean CO_2 mole fraction ~~was 439.7 μmol mol^{-1}~~ during the whole experimental period (March 2013 to August 2015) was 439.7 μmol mol^{-1}, which is 40.6 μmol mol^{-1} higher than the value observed at WLG for the same period. In 2014, the calendar year with complete data coverage, the mean CO_2 mole fraction was 441.2 μmol mol^{-1}, which is 42.5 ppm higher than the WLG value for the same year.

The $^{13}C/^{12}C$ ratio of atmospheric CO_2 displayed a more clear seasonal cycle than the mole fraction (Figure 2). The monthly mean value was (-9.07 ± 0.17) ‰ (mean ± standard error) and (-7.63 ± 0.18) ‰ for January and July, respectively~~(-9.07 ± 0.91) ‰ and (-7.63 ± 0.97 ‰) for January and July, respectively~~, with a seasonal amplitude of 1.44 ‰. The mean value for the whole experimental period was -8.48 ‰, which is the same as the WLG value (-8.48 ‰). The summertime (June to August) $\delta^{13}C$ was 0.39 ‰ higher than the WLG background value. The seasonality of the $^{13}C/^{12}C$ ratio at Nanjing was greater than that at WLG.

The strongest diel variation in the CO_2 mole fraction was observed in the autumn season (September to November) and the weakest in the winter season (December to February), with a diel amplitude of 27.9 μmol mol^{-1} and 13.4 μmol mol^{-1}, respectively (Figure 3). In the summer season, the peak value was observed at 07:00 and the lowest value at 19:00. In cContrastry to the CO_2 mole fraction, $\delta^{13}C$ showed the lowest value in the early morning and the highest value in the afternoon in all the four seasons. The diel amplitude was 1.36 ‰ in the summer and 0.66 ‰ in the winter.

3.2 $^{13}C/^{12}C$ ratio of the surface sources (δ_S)

Figures 4 and 5 show an example of the modified Miller-Tans approach applied to the month of January 2014. According to the slope parameter estimation, the $^{13}C/^{12}C$ ratio of the surface sources was (-25.01 ± 0.90) ‰ (mean ± 95 % confidence limit) for the YRD (Figure 4) and (-25.23 ± 0.74) ‰ for Nanjing (Figure 5).

Figure 6 shows the monthly isotopic ratio calculated with the Miller-Tans method for the whole observation period. The reader is reminded here that the results obtained for the daytime and the nighttime period represent sources in the YRD and in Nanjing, respectively. During the two and a half years of observation, the monthly δ_S for the YRD was lower in the winter [(-24.37 ± 0.71) ‰] and higher in the summer ([(-23.42 ± 1.79) ‰]). The seasonal difference for Nanjing was smaller than for the YRD [(-24.87 ± 0.51) ‰ in the winter (December to February) and -24.80 ± 1.79) ‰ in the summer months (June to August)]. The sources in the YRD had slightly higher δ_S than those in in Nanjing. The mean δ_S value of the whole observational period was (-24.37 ± 0.61) ‰ and (-245.58 ± 0.44) ‰ for the YRD and

Nanjing, respectively. The monthly δ_S for the YRD (Figure 6a) was highly correlated with the monthly atmospheric $\delta^{13}C$ [Figure 2; $\delta_S = (2.29 \pm 0.78)\ \delta^{13}C + (-5.71 \pm 6.37)$, linear correlation coefficient = 0.47, n = 30, $p < 0.01$]. The correlation between the monthly δ_S for Nanjing (Figure 6b) and the monthly atmospheric $\delta^{13}C$ was weak [$\delta_S = (2.39 \pm 0.92)\ \delta^{13}C + (-3.71 \pm 8.07)$, linear correlation coefficient = 0.03, n = 30, $p = 0.87$]. These correlation patterns suggest that atmospheric $\delta^{13}C$ was influenced more by surface sources at the regional scale than at the local (city) scale.

3.3 Inventory data for anthropogenic sources

The emission strength of anthropogenic sources and their $^{13}C/^{12}C$ ratios were calculated with the inventory method and the data found in the literature, as described in section 2.3. In the YRD, coal combustion was by far the largest source of anthropogenic CO_2, contributing 70 % of the overall "fossil-plus" emission (Table 2). Here the "fossil-plus" emission includes contributions from all forms of fossil fuel combustion and from non-cement industrial processes. The second and third largest source were ammonia synthesis and pig iron manufacturing, with fractional contributions of about 9 %. The "fossil-plus" source contribution to the total anthropogenic emission was 91 %, with the remaining 9 % contributed by cement production (Table 2).

In the Nanjing municipality, the fractional contribution of coal to the "fossil-plus" total was 52 %, lower than that for the YRD, and the other three major sources were ammonia synthesis (16 %), pig iron (13 %), and gasoline (11 %). The fractional contribution of fuel-plus sources to the total anthropogenic emission was 96.4 % and the fractional contribution of

412 cement production was 3.6 % (Table 2). The isotopic ratio of the "fossil-plus" sources was
413 0.35 ‰ lower for Nanjing than for the YRD.

414 The overall effective isotopic ratio of the anthropogenic sources weighted by the source
415 contributions was also lower for Nanjing than for the YRD (Table 3). The difference was
416 1.76 ‰ and was a result of lower fractional contributions in Nanjing of coal combustion and
417 cement production, which have relatively high ^{13}C contents, and a higher fractional
418 contribution of natural gas, which is the fuel type with the lowest ^{13}C content.

419

420 **3.4. CO_2 fluxes in YRD and Nanjing**

421 Figure 7 shows the biological flux F_P and surface flux F_S calculated from the mass balance,
422 and the cement flux F_C and "fossil-plus" F_F. The F_P flux obtained with the isotopic
423 partitioning method for the YRD agreed with the seasonal phenology expected for plants in
424 this region. It was near zero or slightly negative in the summer and generally positive in the
425 winter, indicating uptake and release, respectively. The annual mean daytime biological flux
426 was (0.03 ± 0.64) mg m^{-2} s^{-1} in the YRD in the calendar year 2014. The net surface flux F_S
427 was (0.17 ± 2.02) mg m^{-2} s^{-1} in 2014. The standard deviations of these estimates are quite
428 large. If the extreme standard deviations of F_p (5.16 mg m^{-2} s^{-1}) and F_S (22.00 mg m^{-2} s^{-1}) in
429 March 2014 were excluded, the mean standard deviation of F_p would decrease to 0.23 mg m^{-2}
430 $s^{-1}$for and that of F_S to 0.20 mg m^{-2} s^{-1}.

431 In Nanjing, the biological flux was positive throughout the year (Figure 8). This is
432 because the partitioning was done for the night hours when the natural ecosystems were a
433 source of CO_2 due to autotrophic and heterotrophic respiration. The annual mean nighttime

biological flux for the calendar year 2014 was (0.06 ± 0.26) mg m^{-2} s^{-1}. The nighttime surface flux was (0.18 ± 0.22) mg m^{-2} s^{-1} in 2014.

4 Discussion

4.1 CO_2 mole fraction and $\delta^{13}C$ seasonality

The atmospheric CO_2 mole fraction observed in Nanjing showed very small seasonal variation (summer versus winter difference of 7.9 μmol mol^{-1}, July versus January difference of 15.6 μmol mol^{-1}), in comparison with the data published for other cities. For example, ~~The CO_2 mole fraction difference between the cold and the warm season is about 66 μmol mol^{-1} in Phoenix, USA (Idso et al. 2002). I~~In Salt Lake City, USA, the CO_2 mole fraction in the summer is about 31 μmol mol^{-1} lower than in the winter (Pataki et al., 2003). ~~In Chicago, USA, the CO_2 mole fraction varied from 397 μmol mol^{-1} in August 2011 to 427 μmol mol^{-1} in January 2012, showing a seasonal amplitude of 30 μmol mol^{-1} (Moore and Jacobson 2015). In Beijing, China, the seasonal variation of atmospheric CO_2 mole fraction is about 64.5 μmol mol^{-1} (August versus January; Pang et al. 2016). However, a similar small seasonal amplitude of 5 μmol mol^{-1} CO_2 was observed in Pasadena, USA during 2006 to 2013, which was consistent with the seasonal variation of background and transport of emissions from fossil fuel combustion (Newman et al. 2016).~~

Several factors contributed to the weak seasonality in Nanjing. The climate in the YRD is relatively mild. The governmental energy policy prohibits winter heating in public buildings. Most residential buildings also lack space heating in the winter. This is in contrast to energy use patterns in northern cities in China and elsewhere. ~~In London, UK, natural gas usage in~~

Formatted: Indent: First line: 0 ch

~~the winter heating season is 29 % greater than in the non-heating autumn season (Helfter et al. 2011). In Salt Lake City, USA, energy consumption in the winter was 41 % greater than in the summer (Bush et al, 2007). A similar seasonal trend of energy consumption has also been reported for Beijing (Pang et al, 2016). In Chicago, natural gas usage comprises 70 % to 80 % of total fossil fuel consumption in the winter and about 50 % in the summer (Moore and Jacobson 2015). The weak energy use seasonality in the YRD partially explains why the observed CO_2 mole fraction had a smaller seasonal amplitude (Figure 2) than reported for other northern cities.~~

The weak seasonality of the observed mole fraction was also related to the low vegetation cover in the YRD and in Nanjing. The forest cover ratio is about 35 % in Nanjing and in the YRD, and the overall vegetation cover (forest plus other vegetation types) ratio in the major cities in the YRD is lower than 45 % (CESY, 2013; CSY, 2013). For comparison, the vegetation cover ratio is 56 % in Salt Lake City (Pataki et al. 2009) and 44 % in Chicago (Rose et al. 2003). Dense vegetation is known to deplete atmospheric CO_2 in the summer season via photosynthetic uptake, amplifying the CO_2 seasonal amplitude.

Our $\delta^{13}C$ seasonal amplitude (January versus July difference of 1.44 ‰) was 4 times the amplitude observed or estimated at WLG (Figure 2) but agreed with those reported by most urban studies. For comparison, the seasonal amplitude of $\delta^{13}C_a$ in Bangalore, India, was 0.89 to 1.32 ‰ (Guha and Ghosh 2015). Similar amplitudes have also been reported for Chicago (January versus August difference of 1.25 ‰; Moore and Jacobson, 2015) and Beijing (2.13 ‰; Pang et al. 2016). In Salt Lake City, the seasonal amplitude of $\delta^{13}C$ was

477 approximately 1.6 ‰ because of much more natural gas consumption for heating in the
478 winter than in the summer (Pataki et al. 2006).
479
480 **4.2 Influences of cement production on atmospheric $\delta^{13}C$**
481 The high summer $\delta^{13}C$ was one of the most unique characteristics at our site. The daytime
482 $\delta^{13}C$ reached -6.90 ‰ in July 2013 and -7.21 ‰ in August 2014, which were 1.28 ‰ and
483 0.95 ‰ higher than the WLG values. The highest monthly mean $\delta^{13}C$ occurred in July: -
484 7.44 ‰ in July 2013, -7.99 ‰ in July 2014 and -7.46 ‰ in July 2015. These values were
485 0.74 ‰, 0.16 ‰ and 0.77 ‰ higher than the WLG value reported for the same months.
486 The high July values observed at our site cannot be fully explained by CO_2 removal by
487 plant photosynthesis. Photosynthesis and respiration are the two processes that dominate the
488 $^{13}C/^{12}C$ seasonality in plant-dominated landscapes, leading to higher $\delta^{13}C$ values in the
489 summer and lower values in the winter. For example, in Park Falls, Wisconsin, USA, a site in
490 a heavily-forested landscape, $\delta^{13}C$ was -7.75 ‰ in August 2011 and -8.77 ‰ in February
491 2012 (Moore and Jacobson, 2015). For comparison, $\delta^{13}C$ was -8.24‰ and -8.38 ‰ at the
492 Mauna Loa Observatory and -8.02 ‰ and -8.66 ‰ at WLG in these two months, respectively.
493 In other words, the photosynthetic effect raised the August $\delta^{13}C$ by 0.5 ‰ above the
494 background value, a smaller enrichment than observed at our site. Because of the low
495 vegetation fraction, the summer photosynthetic CO_2 uptake in the YRD and in Nanjing
496 should be lower than at Park Falls. According to the CarbonTracker inversion analysis (Peters
497 et al. 2007), the net ecosystem production at the grid point where Parks Fall is located is -
498 0.201 mg m^{-2} s^{-1} in July, 2014 but is only -0.059 mg m^{-2} s^{-1} at the grid point corresponding to

499 the YRD region. We would expect from the photosynthetic effect alone that the summertime
500 ^{13}C enrichment at our site to be smaller, not greater than that observed at Park Falls.
501 Furthermore, in a human-dominated landscape, the plant photosynthetic enhancement of
502 ^{13}C is offset by the CO_2 from fossil fuel combustion which has lower $^{13}C/^{12}C$ ratios than the
503 atmosphere. In Chicago, the monthly mean $\delta^{13}C$ peaked in August at -8.29 ‰ during the
504 calendar year 2011, which is 0.05 ‰ lower than the WLG value for the same month.
505 Similarly, in Beijing, the monthly mean $\delta^{13}C$ peaked at -9.49 ‰ in August 2014, which is
506 1.23 ‰ lower than the WLG value for the same month.
507 We suggest that cement production was the contributing factor responsible for the high
508 $\delta^{13}C$ values in the summer. The evidence supporting this interpretation is provided by data in
509 Table 3 and Figure 7. The delta value of anthropogenic CO_2 in the YRD would be (-26.36 ±
510 0.42) ‰ without cement production and increased to (-23.95 ± 0.41) ‰ after inclusion of the
511 cement source (Table 3). This ~~δ_{delta} C~~ value is much higher than those reported for other urban
512 lands, such as -30.7 ‰ for Los Angeles, USA (Newman et al. 2008) and about -31 ‰ for Salt
513 Lake City, USA (Bush et al. 2007). The overall surface source $^{13}C/^{12}C$ ratio derived from
514 atmospheric measurements (Figure 6; -24.37 ‰ and -24.58 ‰ for the YRD and Nanjing,
515 respectively) was also more enriched than those obtained from atmospheric measurements in
516 other cities, such as (-28.1 ± 0.8) ‰ for Chicago in August and September (Moore and
517 Jacobson, 2015), -32.4 ‰ to -27.4 ‰ for Salt Lake City in the growing season (Pataki et al.
518 2003), -27.0 ‰ for Beijing in the winter heating season (Pang et al. 2016), and -29.3 ‰ for
519 Los Angeles, USA (Newman et al. 2008).

Formatted: Font: Symbol
Formatted: Subscript

520 The influence of cement production on atmospheric $\delta^{13}C$ has also been suggested for at
521 least two other urban sites. In Bangalore, India, $\delta^{13}C$ is 0.05 ‰ higher than that observed at
522 an island station in the Indian Ocean, and cement production in southern India is offered as a
523 reason to explain the enrichment of urban $\delta^{13}C$ (Guha and Ghosh 2015). The other urban site
524 is Beijing, China, where the $\delta^{13}C$ measurement may have been influenced by cement factories
525 outside the city (Ren et al. 2015, Pang et al. 2016).
526
527 **4.3 Net surface and biological fluxes in the YRD**
528 As a human-dominated landscape, the YRD was a net source of CO_2 on the monthly scale
529 even in the growing season (F_S, Figure 7). The seasonal trends of the net surface flux F_S and
530 the biological flux F_P were highly correlated with each other ($R^2 = 0.88$ after exclusion of
531 three extreme outliers) because the anthropogenic source strengths were almost constant. The
532 mean F_S between March 2013 and February 2015 was (0.19 ± 1.16) mg m^{-2} s^{-1}, which
533 consisted of (0.15 ± 0.02) mg m^{-2} s^{-1} from fossil combustion and industrial processes, (0.02 ±
534 0.002) mg $m^{-2}s^{-1}$ from cement production and (0.05 ± 1.31) mg m^{-2} s^{-1} from biological
535 activities. The total anthropogenic CO_2 flux was (0.17± 0.02) mg m^{-2} s^{-1} in the YRD, a 70 %
536 increase from the value of 0.10 mg m^{-2} s^{-1} reported for 2009 (Shen et al. 2014). From 2009 to
537 2012, the GDP increased by 56 % according to the National Statistic Yearbook.
538 For comparison, we extracted the flux data from the CarbonTracker database for the 6
539 by 6 pixels that cover the YRD region. The results show that the mean daytime (11:00 to
540 17:00 local time) biological flux is slightly negative at -0.01 mg m^{-2} s^{-1} for 2014 (Peter et al.
541 2007). Our estimate of F_P for 2014 was (0.03 ± 0.64) mg m^{-2} s^{-1}. As pointed out earlier, the F_p

Formatted: Superscript

542 value for March 2014 was highly uncertain [(0.21± 5.16) mg m^{-2} s^{-1}]; If we replace this value
543 by the mean value of February and April 2014, the 2014 mean F_P would be reduced to (0.02 ±
544 0.22) mg m^{-2} s^{-1}.

545 A source of uncertainty in our flux partitioning analysis is related to human breath (Affek
546 and Eiler 2006). Using the method of Prairie and Duarte (2007), we estimated that human
547 respiration flux was 0.006 and 0.013 mg m^{-2} s^{-1}, or 3.7 % and 11.65 % of anthropogenic
548 emission in the YRD and in Nanjing, respectively. The food diet in the region is
549 predominantly C3 grains. By including this additional source in Equations 3 and 4 and by
550 assuming that the isotopic ratio of ~~human respiration~~digestion is the same as δ_P shown in
551 Table 3, F_S and F_P would increase by 0.008 and 0.001 mg m^{-2} s^{-1} in the YRD and by 0.018 mg
552 m^{-2} s^{-1} and 0.005 mg m^{-2} s^{-1} in Nanjing, respectively.
553
554 **4.4 Comparison of the Miller-Tans and the Keeling methods**
555 By applying the Miller-Tans method to daytime and nighttime observations separately, we
556 obtained the effective source ratios that are consistent with the inventory analysis for the
557 YRD and for the Nanjing Municipality. The daytime measurement (Figure 6a, solid circles)
558 revealed that the $^{13}C/^{12}C$ ratio of the all sources (anthropogenic and biological) w~~er~~as~~e~~ on
559 average 0.21 ‰ higher than that obtained with the nighttime measurement (Figure 6b, solid
560 circles), although the difference is not statistically significant (p = 0.38). For comparison, the
561 overall δ_S of the anthropogenic sources in the YRD was also higher than that in Nanjing, the
562 difference being 2.01 ‰ (Table 3~~2~~). The interpretation that the daytime observations capture
563 the influence of surface sources in the YRD region is supported by a trajectory analysis and

Formatted: Font: Italic

564 by an analysis of the atmospheric methane to CO_2 emissions ratio observed at the same site
565 (Shen et al. 2014). We note that the atmospheric measurements gave a smaller difference
566 between the YRD and Nanjing than that obtained by the inventory data, likely because of
567 different biological contributions between the two spatial scales.
568 One open question with regard to the modified Miller-Tans method is what constitutes
569 the true background air for the YRD. In this study, the background was assumed to be the
570 tropospheric air above the YRD. The background delta value (δ_b) backed out from the
571 intercepts shown in Figures 4 and 5 is -7.6 ‰, which is higher than expected, suggesting that
572 the true background concentration C_b may be higher than the tropospheric value. One
573 noteworthy feature about Equation 3 is that its slope parameter is not sensitive to C_b, but its
574 intercept parameter is. By increasing C_b by 15 μmol mol^{-1}, the slope of the regression in
575 Figure 5 would remain unchanged, but the δ_b backed out from the new intercept value would
576 become more reasonable (-8.23 ‰). In Newman et al. (2016), the background air was
577 measured at a coastal location upwind of the Los Angles airshed. It is recommended that a
578 similar strategy should be used in future experiments, where simultaneous measurement is
579 made at the coast of East China Sea and only data collected in easterly winds are selected for
580 the Miller-Tans analysis.
581 We also calculated the $^{13}C/^{12}C$ ratio of the surface sources with the Keeling plot method.
582 Using the daytime data, the Keeling result was lower and more variable than that inferred
583 from the Miller-Tans method using the daytime data (Figure 6a). The two methods differed
584 by an average of -1.51 ‰ (Supplementary Table S2).

Formatted: Font color: Text 1
Formatted: Font: Symbol
Formatted: Subscript
Formatted: Font color: Text 1
Formatted: Font color: Text 1
Formatted: Subscript
Formatted: Font: Symbol
Formatted: Superscript
Formatted: Font color: Auto

In comparison, the Keeling plot method showed reasonably good performance when applied to the nighttime observations. This is because surface inversion conditions effectively prevented mixing of the free atmospheric air with the surface air, so that the single-source assumption implicit in the Keeling plot method could be satisfied. When~~If~~ we applied Keeling plot method at monthly intervals to the nighttime data, the resulting δ_S showed very similar month-to-month variations with the value obtained with application of the Miller-Tans method to the nighttime observations (Figure 6b). The two method differed by an average of 1~~0~~.21 ‰ (Supplementary Table S2).

When the δ_S derived from the Keeling plot method was used for flux-partitioning, the results were much more erratic than shown in Figures 7 and 8 (Supplementary Figures S3 and S4). The uncertainty ranges of the monthly F_P and F_S were two to three times larger. The biological flux F_P for the YRD was out of range for 4 months, and did not display an obvious seasonal pattern (Supplementary Figure S3). These results support our choice of the modified Miller-Tans method as the preferred approach for inferring the overall $^{13}C/^{12}C$ ratio of the surface sources in this study.

Formatted: Font: Symbol
Formatted: Subscript
Formatted: Subscript
Formatted: Subscript
Formatted: Superscript
Formatted: Superscript

5. Conclusion

We showed that the temporal changes of $\delta^{13}C$ followed the seasonal patterns of anthropogenic and biologic CO_2 emissions, with lower values in the winter than in the summer. An unusual feature that has not been seen in other urban environments is that the $\delta^{13}C$ exceeded that of the background atmosphere in some of the summer months. The highest monthly $\delta^{13}C$ was -7.44 ‰ observed in July 2013, which was 0.74 ‰ greater than the

607 WLG value for the same month. Evidence points to cement production as the key reason for
608 why the atmospheric $\delta^{13}C$ was higher than at the background site. In contrast to the isotope
609 ratio, the CO_2 mole fraction displayed very weak seasonality (July to January difference 15.6
610 μmol mol^{-1}).

611 We hypothesized that the Miller-Tans method applied to the daytime and nighttime
612 observations should yield the effective $^{13}C/^{12}C$ ratio of surface sources at the regional (YRD)
613 and the local (Nanjing) scale, respectively. According to the results of the modified Miller-
614 Tans method, the effective source $^{13}C/^{12}C$ ratio in the YRD was -24.37 ‰, which was 0.21 ‰
615 higher than that in the Nanjing Municipality. These results were consistent with inventory
616 estimates of anthropogenic source ratios at these two spatial scales.

617 By combining inventory data on anthropogenic carbon sources and the atmospheric
618 measurement of CO_2 mole fraction and $^{13}C/^{12}C$ ratio in an isotopic partitioning framework,
619 we inferred that natural ecosystems in the YRD were a negligibly small source of
620 atmospheric CO_2, with an average flux of (0.02 ± 0.22) mg m^{-2} s^{-1} for 2014. For comparison,
621 the CarbonTracker inverse analysis reveals a small annual mean daytime biological flux (-
622 0.01 mg m^{-2} s^{-1}) for this region for 2014.

623

624 **Data availability：**

625 The atmospheric data are available upon request and from the Yale-NUIST Center website
626 http://yncenter.sites.yale.edu/publications.

627

628 **Acknowledgments:**

This research was supported by the National Natural Science Foundation of China (Grant 41475141, 41505005), the U. S. National Science Foundation (Grant 1520684), the Ministry of Education of China (Grant PCSIRT), and the Priority Academic Program Development of Jiangsu Higher Education Institutions (Grant PAPD). The first author also acknowledged a visiting scholarship from China Scholarship Council and a Graduate Student Innovation Grant from Jiangsu Provincial Government (Grant KYLX_0848). We thank the handling editor Dr. Jan Kaiser and four~~three~~ anonymous reviewers whose constructive comments have greatly improved this paper.

References

Affek, H. P., Eiler, J. M. (2006). Abundance of mass 47-CO_2 in urban air, car exhaust, and human breath. Geochimica et Cosmochimica Acta **70**(1): 1-12.

Akbari H, Menon S, Rosenfeld A. Global cooling: increasing world-wide urban albedos to offset CO_2. Climatic Change, 2009, **94**(3-4): 275-286.

An, H (2012) Ammonia synthesis: current status and future outlook (in Chinese), Coal Chemsitry of Western China, **2**: 4-13.

Andres, R. J., Marland, G., Boden, T., Bischof, S. (1994). Carbon dioxide emissions from fossil fuel consumption and cement manufacture, 1751-1991; and an estimate of their isotopic composition and latitudinal distribution, Oak Ridge National Lab., TN (United States);

Bai, Y., (2011) A Comparative Study on Turbulent Fluxes Exchange over Nanjing Urban and Suburban in Summer (in Chinese), Master's Thesis, Nanjing University of Information Science & Technology.

Ballantyne, A. P., Miller, J. B., Baker, I. T., Tans, P. P., White, J. W. C. (2011). Novel applications of carbon isotopes in atmospheric CO_2: what can atmospheric measurements teach us about processes in the biosphere? Biogeosciences, 8(10), 3093-3106.

Ballantyne, A. P., Miller, J. B., Tans, P. P. (2010). Apparent seasonal cycle in isotopic discrimination of carbon in the atmosphere and biosphere due to vapor pressure deficit. Global Biogeochemical Cycles, 24(3), 1-16.

Bowling, D. R., S P Burns, T. J. Conway, R. K. Monson, and J. W. C. White (2005) Extensive observations of CO_2 carbon isotope content in and above a high-elevation subalpine forest, Global Biogeochemical Cycles, **19**: GB3023.

Bi, J., Zhang, R., Wang, H., Liu, M.,Wu, Y. (2011). The benchmarks of carbon emissions and policy implications for China's cities: Case of Nanjing. Energy Policy **39**(9): 4785-4794.

Bowling, D. R., Sargent, S. D., Tanner, B. D., and Ehleringer, J. R. (2003). Tunable diode laser absorption spectroscopy for stable isotope studies of ecosystem–atmosphere CO_2 exchange, Agric. Forest Meteorol., **118:** 1–19.

Bush, S. E., Pataki, D.E., Ehleringer, J.R. (2007). Sources of variation in $\delta^{13}C$ of fossil fuel emissions in Salt Lake City, USA. Applied Geochemistry **22**(4): 715-723.

CESY (2013). China Energy Statistical Yearbook 2013: China Statistical Publishing House, Beijing. (in Chinese) Also available at: <http://www.stats.gov.cn/tjsj/ndsj/2013/indexch.htm>.

Clark-Thorne, S. T., C. J. Yapp (2003). Stable carbon isotope constraints on mixing and mass balance of CO2 in an urban atmosphere: Dallas metropolitan area, Texas, USA. Applied Geochemistry **18**(1): 75-95.

Coutts, A. M., Beringer, J., Tapper, N.J. (2007). Characteristics influencing the variability of urban CO_2 fluxes in Melbourne, Australia. Atmospheric Environment **41**(1): 51-62.

China Cement: http://hy.ccement.com/map/, last access: 6 July 2016 (in Chinese).

CSY (2013). China Statistical Yearbook. National Bureau of Statistics of China. (in Chinese) Also available at: <http://www.stats.gov.cn/tjsj/ndsj/2013/indexch.htm>

Duan Y. (1995) Study of characteristics of coal isotope conposition in China. Coal Geology & Exploration **23**(1) 29-33.

Ehleringer, J.R., Bowling, D.R., Flanagan, L.B., Fessenden, J.,Helliker, B., Martinelli, L.A., Ometto, J.P. (2002). Stable isotopes and carbon cycle processes in forests and grasslands. Plant biology **4**(2): 181-189.

Farquhar, G., J. Lloyd (1993). Carbon and oxygen isotope effects in the exchange of carbon dioxide between terrestrial plants and the atmosphere. Stable isotopes and plant carbon-water relations **40**: 47-70.

Fessenden, J. E., J. R. Ehleringer (2002). Age-related variations in $\delta^{13}C$ of ecosystem respiration across a coniferous forest chronosequence in the Pacific Northwest. Tree Physiology **22**(2-3): 159-167.

Friedman, L., A. P. Irsa (1967). Variations in isotopic composition of carbon in urban atmospheric carbon dioxide. Science **158**(3798): 263-264.

Gorski G, Strong C, Good S P, Bares, R., Ehleringer, J. R., Bowen, G. J. (2015). Vapor hydrogen and oxygen isotopes reflect water of combustion in the urban atmosphere. Proceedings of the National Academy of Sciences, **112**(11): 3247-3252.

Griffis, T. J., Lee, X., Baker, J.M., Sargent, S.D., King, J.Y. (2005). Feasibility of quantifying ecosystem–atmosphere $C^{18}O^{16}O$ exchange using laser spectroscopy and the flux-gradient method. Agricultural and Forest Meteorology, **135**(1-4): 44-60.

Griffis, T J. (2013). Tracing the flow of carbon dioxide and water vapor between the biosphere and atmosphere: A review of optical isotope techniques and their application. Agricultural and Forest Meteorology, **174**:85-109.

Guha, T., P. Ghosh (2010). Diurnal variation of atmospheric CO_2 concentration and delta C-13 in an urban atmosphere during winter-role of the nocturnal boundary layer. Journal of Atmospheric Chemistry, **65**(1): 1-12.

Guha, T. and P. Ghosh (2015). Diurnal and seasonal variation of mixing ratio and delta C-13 of air CO_2 observed at an urban station Bangalore, India. Environmental Science and Pollution Research, **22**(3): 1877-1890.

~~Helfter, C., Famulari, D., Phillips, G.J., Barlow, J.F., Wood, C.R.,Grimmond, C.S.B., Nemitz, E. (2011). Controls of carbon dioxide concentrations and fluxes above central London. Atmospheric Chemistry and Physics **11**(5): 1913-1928.~~

ICLEI (International Council for Local Environmental Initiatives). (2008). Local government operations protocol for the quantification and reporting of greenhouse gas emissions inventories. [Available online at http://www.arb.ca.gov/cc/protocols/localgov/archive/final lgo protocol 2008–09–25.pdf.]

Jasechko, S., Gibson, J. J., Edwards, T. W. (2014). Stable isotope mass balance of the Laurentian Great Lakes. Journal of Great Lakes Research, **40**(2), 336-346.

~~Idso, S. B., Idso, C.D., Balling, R.C. (2002). Seasonal and diurnal variations of near-surface atmospheric CO_2 concentration within a residential sector of the urban CO_2 dome of Phoenix, AZ, USA. Atmospheric Environment, **36**(10): 1655-1660.~~

Jasek, A., Zimnoch, M., Gorczyca, Z., Smula, E., Rozanski, K. (2014). Seasonal variability of soil CO2 flux and its carbon isotope composition in Krakow urban area, Southern Poland. Isotopes in Environmental and Health Studies, **50**(2): 143-155.

Keeling, C. D. (1958). The concentration and isotopic abundances of atmospheric carbon dioxide in rural areas. Geochimica et Cosmochimica Acta, **13**(4): 322-334.

Keeling, C. D. (1961). The concentration and isotopic abundances of carbon dioxide in rural and marine air. Geochimica et Cosmochimica Acta, **24**(3): 277-298.

Koerner, B., J. Klopatek (2002). Anthropogenic and natural CO_2 emission sources in an arid urban environment. Environmental Pollution, **116**: S45-S51.

Leavitt, S. W., Paul, E.A., Galadima, A., Nakayama, F.S., Danzer, S.R., Johnson, H., Kimball, B.A. (1995). Carbon isotopes and carbon turnover in cotton and wheat FACE experiments. Plant and Soil **187**(2): 147-155.

Formatted: Indent: Left: 0"

Formatted: Indent: Left: 0"

Formatted: Indent: Left: 0"

Lee, X., Sargent, S., Smith, R., & Tanner, B. (2005). In situ measurement of the water vapor $^{18}O/^{16}O$ isotope ratio for atmospheric and ecological applications. Journal of Atmospheric and Oceanic Technology, **22**(5), 555-565.

Lichtfouse, E., Lichtfouse, M., Jaffrezic, A. (2003). delta C-13 values of grasses as a novel indicator of pollution by fossil-fuel-derived greenhouse gas CO_2 in urban areas. Environmental Science & Technology, **37**(1): 87-89.

Liu, H., Feng, J., Järvi, L., Vesala, T. (2012). Four-year (2006–2009) eddy covariance measurements of CO_2 flux over an urban area in Beijing. Atmospheric Chemistry and Physics, **12**(17): 7881-7892.

Lloyd, J., Kruijt, B., Hollinger, D.Y., Grace, J., Francey, R.J., Wong, S., Kelliher, F.M., Miranda, A.C., Farquhar, G.D., Gash, J.H.C. (1996). Vegetation effects on the isotopic composition of atmospheric CO_2 at local and regional scales: theoretical aspects and a comparison between rain forest in Amazonia and a boreal forest in Siberia. Functional Plant Biology, **23**(3): 371-399.

Lloyd, J., Francey, R.J., Mollicone, D., Raupach, M.R, Sogachev, A., Arneth, A., Byers, J.N., Kelliher, F.M., Rebmann, C., Valentini, R. (2001). Vertical profiles, boundary layer budgets, and regional flux estimates for CO_2 and its $^{13}C/^{12}C$ ratio and for water vapor above a forest/bog mosaic in central Siberia. Global Biogeochemical Cycles, **15**(2): 267-284.

McDonald, B.C., McBride, Z. C., Martin, E. W., Harley, R. A. (2014). High-resolution mapping of motor vehicle carbon dioxide emissions. Journal of Geophysical Research: Atmospheres, **119**(9): 5283-5298.

McManus, J. B., Zahniser, M.S., Nelson, D.D., Williams, L.R., Kolb, C.E. (2002). Infrared laser spectrometer with balanced absorption for measurement of isotopic ratios of carbon gases. Spectrochimica Acta Part A: Molecular and Biomolecular Spectroscopy, **58**(11): 2465-2479.

Miller, J. B., P. P. Tans (2003). Calculating isotopic fractionation from atmospheric measurements at various scales, Tellus B, **55**(2): 207-214.

Miller, J.B., Tans, P.P., White, J.W.C., Conway, T.J., Vaughn, B.W. (2003). The atmospheric signal of terrestrial carbon isotopic discrimination and its implication for partitioning carbon fluxes, Tellus B, **55**(2): 197-206.

~~Newman, S., Xu, X., Gurney, K.R., Hsu, Y.K., Li, K.F., Jiang, X., Keeling, R., Feng, S., O'Keefe, D., Patarasuk, R. and Wong, K.W. (2016). Toward consistency between trends in bottom-up CO_2 emissions and top-down atmospheric measurements in the Los Angeles megacity. Atmospheric Chemistry and Physics, **16**(6):3843-3863.~~

Moore J., Jacobson A.D. (2015). Seasonally varying contributions to urban CO_2 in the Chicago, Illinois, USA region: Insights from a high-resolution CO_2 concentration and $d^{13}C$ record. Elementa: Science of the Anthropocene, **3**: 000052.

Mu, H., Li, H., Zhang, M., Li, M. (2013). Analysis of China's carbon dioxide flow for 2008. Energy Policy **54**: 320-326.

Newman, S., Xu, X., Gurney, K.R., Hsu, Y.K., Li, K.F., Jiang, X., Keeling, R., Feng, S., O'Keefe, D., Patarasuk, R. and Wong, K.W. (2016). Toward consistency between trends in bottom-up CO_2 emissions and top-down atmospheric measurements in the Los Angeles megacity. Atmospheric Chemistry and Physics, **16**(6):3843-3863.

Newman, S., Xu, X., Affek, H.P., Stolper, E., Epstein, S. (2008). Changes in mixing ratio and isotopic composition of CO2in urban air from the Los Angeles basin, California, between 1972 and 2003, Journal of Geophysical Research, **113**(D23): 1-15.

NSY (2013). Nanjing Statistical Yearbook. Nanjing Municipal Bureau Statistics. (in Chinese) Also available at: < http://www.njtj.gov.cn/2004/2013/renmin/index.htm>

Ometto, J. P., Flanagan, L.B., Martinelli, L.A., Moreira, M.Z., Higuchi, N., Ehleringer, J.R. (2002). Carbon isotope discrimination in forest and pasture ecosystems of the Amazon Basin, Brazil, Global Biogeochemical Cycles, **16**(4):1-10.

Ometto, J.P., Ehleringer, J.R., Domingues, T.F., Berry, J.A., Ishida, F.Y., Mazzi, E., Higuchi, N., Flanagan, L.B., Nardoto, G.B., Martinelli, L.A. (2006). The stable carbon and nitrogen isotopic composition of vegetation in tropical forests of the Amazon Basin, Brazil, Biogeochemistry, **79**(1-2): 251-274.

Pan, J. (2007) Theoretical and Process Studies of the Abatement of Fuel Gas Emissions during Iron Ore Sintering (in Chinese), PhD Dissertation, Southcentral Univeristy of China.

Pang, J., Wen, X., Sun, X. (2016). Mixing ratio and carbon isotopic composition investigation of atmospheric CO_2 in Beijing, China. Sci Total Environ, **539**: 322-330.

~~Pataki, D. E. (2005). Can carbon dioxide be used as a tracer of urban atmospheric transport? Journal of Geophysical Research **110**(D15102): 1-8.~~

Pataki, D. E., Bowling, D.R., Ehleringer, J.R. (2003). Seasonal cycle of carbon dioxide and its isotopic composition in an urban atmosphere: Anthropogenic and biogenic effects. Journal of Geophysical Research-Atmospheres, **108**(D23): 1-8.

Pataki, D. E., Bowling, D.R., Ehleringer, J.R., Zobitz, J.M. (2006). High resolution atmospheric monitoring of urban carbon dioxide sources. Geophysical Research Letters, **33**(3): 1-5.

Pataki, D. E., Ehleringer, J.R., Flanagan, L.B., Yakir, D., Bowling, D.R., Still, C.J., Buchmann, N., Kaplan, J.O., Berry, J.A. (2003). The application and interpretation of Keeling plots in terrestrial carbon cycle research. Global Biogeochemical Cycles, **17**(1): 1-14

Pataki, D. E., Lai, C., Keeling, C.D., Ehleringer, J.R. (2007). Insights from stable isotopes on the role of terrestrial ecosystems in the global carbon cycle. Terrestrial Ecosystems in a Changing World, Springer: 37-44.

Pataki,D.E., Emmi,P.C., Forster,C.B., Mills,J.I., Pardyjak,E.R., Peterson,T.R., Thompson,J.D., Dudley-Murphy,E., An integrated approach to improving fossil fuel emissions scenarios with urban ecosystem studies. Ecological Complexity, 2009, **6**(1): 1-14.

~~Pataki, D. E., Xu, T., Luo, Y.Q., Ehleringer, J.R. (2007). Inferring biogenic and anthropogenic carbon dioxide sources across an urban to rural gradient. Oecologia **152**(2): 307-322.~~

Peters,W., Jacobson, A.R., Sweeney, C., Andrews, A.E., Conway, T.J., Masarie, K., Miller, J.B., Bruhwiler, L.M., Petron, G., Hirsch, A.I., Worthy, D.E., van der Werf, G.R., Randerson, J.T., Wennberg, P.O., Krol, M.C., Tans, P.P. (2007) An atmospheric perspective on North American carbon dioxide exchange: CarbonTracker, Proceedings of the National Academy of Sciences, **104**(48): 18925-18930.

Prairie, Yves T., Duarte, C. M. (2007). Direct and indirect metabolic CO_2 release by humanity. Biogeosciences, **4**(2): 215-217.

Rella, C. (2011). Accurate stable carbon isotope ratio measurements with rapidly varying carbon dioxide concentrations using the Picarro $\delta^{13}C$ G2101-i gas analyzer, Picarro White Paper. Picarro Inc.

Ren, L., Wang, W., Wang, J., Liu, R. (2015). Analysis of energy consumption and carbon emission during the urbanization of Shandong Province, China. Journal of Cleaner Production, **103**: 534-541.

Röckmann1 T, S Eyer, C. van der Veen1, ME Popa, B Tuzson, G Monteil1, S Houweling, Eliza Harris, D Brunner, H Fischer, G Zazzeri, D Lowry, EG Nisbet, WA Brand, JM Necki, L Emmenegger, and J Mohn (2016). In situ observations of the isotopic composition of methane at the Cabauw tall tower site. Atmos. Chem. Phys., **16**: 10469–10487.

Rose L S, Akbari H, Taha H. Characterizing the fabric of the urban environment: a case study of Greater Houston, Texas. Lawrence Berkeley National Laboratory, 2003.

Formatted: Indent: Left: 0"

Satterthwaite D. Cities' contribution to global warming: notes on the allocation of greenhouse gas emissions. Environment and Urbanization, 2008, **20**(2): 539–549.

Shen, S., Yang, D., Xiao, W., Liu, S., Lee, X. (2014). Constraining anthropogenic CH_4 emissions in Nanjing and the Yangtze River Delta, China, using atmospheric CO_2 and CH_4 mixing ratios, Advances in Atmospheric Sciences, **31**(6): 1343-1352.

Song, T., Wang Y. (2012). Carbon dioxide fluxes from an urban area in Beijing. Atmospheric Research, **106**: 139-149.

Sun, B., Dilcher, D.L., Beerling, D.J., Zhang, C., Yan, D., Kowalski, E. (2003). Variation in Ginkgo biloba L. leaf characters across a climatic gradient in China. Proceedings of the National Academy of Sciences, **100**(12): 7141-7146.

Takahashi, H. A., Konohira, E., Hiyama, T., Minami, M., Nakamura, T., Yoshida, N. (2002). Diurnal variation of CO_2 concentration, Delta C-14 and delta C-13 in an urban forest: estimate of the anthropogenic and biogenic CO_2 contributions, Tellus B, **54**(2): 97-109.

Tans, P. (1981). $^{13}C/^{12}C$ of industrial CO^2. In SCOPE 16: Carbon Qcle Modelling (B.Bolin, ed.), John Wiley and Sons, Chichester, England, 127-129.

Thoning, K. W., Tans, P.P., Komhyr, W.D. (1989). Atmospheric carbon dioxide at Mauna Loa Observatory: 2. Analysis of the NOAA GMCC data, 1974–1985. Journal of Geophysical Research, **94**(D6): 8549-8565.

~~Turnbull, J. C., Sweeney, C., Karion, A., Newberger, T., Lehman, S. J., Tans, P.P., Davis, K.J., Lauvaux, T., Miles, N.L., Richardson, S.J., Cambaliza. (2015). Toward quantification and source sector identification of fossil fuel CO_2 emissions from an urban area: Results from the INFLUX experiment. Journal of Geophysical Research, 120(1): 292-312.~~

Sanam Noreen Vardag, S. N., S. Hammer, I. Levin (2016) Evaluation of 4 years of continuous $^{13}C(CO_2)$ data using a moving Keeling plot method, Biogeosciences, Biogeosciences, **13**: 4237–4251.

Wada, R., Nakayama, T., Matsumi, Y., Hiyama, T., Inoue, G., Shibata, T. (2011). Observation of carbon and oxygen isotopic compositions of CO_2 at an urban site in Nagoya using Mid-IR laser absorption spectroscopy. Atmospheric Environment, **45**(5): 1168-1174.

Wang, D. (2013) Method and Empirical Research of Urban Greenhouse Gas Measurement (in Chinese), Master's Thesis, Tianjin University.

Wang, W. , D. E. Pataki (2012). Drivers of spatial variability in urban plant and soil isotopic composition in the Los Angeles basin. Plant and Soil, **350**(1-2): 323-338.

939 Wen, X. F., Meng, Y., Zhang, X., Sun, X., Lee, X. (2013). Evaluating calibration strategies
940 for isotope ratio infrared spectroscopy for atmospheric $^{13}CO_2/^{12}CO_2$ measurement.
941 Atmospheric Measurement Techniques, **6**(1): 795-823.
942
943 Wehr, R., and S. R. Saleska (2017) The long-solved problem of the best-fit straight line:
944 application to isotopic mixing lines, Biogeosciences, **14**: 17-29.
945
946 Widory, D. (2006). Combustibles, fuels and their combustion products: A view through
947 carbon isotopes. Combustion Theory and Modelling, **10**(5): 831-841.
948
949 Widory, D., M. Javoy (2003). The carbon isotope composition of atmospheric CO_2 in Paris.
950 Earth and Planetary Science Letters, **215**(1-2): 289-298.
951
952 Yakir, D., L. da SL Sternberg (2000). The use of stable isotopes to study ecosystem gas
953 exchange. Oecologia, **123**(3): 297-311.
954
955 Yang, H.M., Wang, H.Z. , Wu, Y.B. (2011). Observation and characteristics analysis of traffic
956 flow in Nanjing. (in Chinese), Environmental Science and Technology, **24**(2): 98-101.
957
958 Zimnoch, M., Florkowski, T., Necki, J., Neubert, R. (2004). Diurnal variability of delta C-13
959 and delta O-18 of atmospheric CO_2 in the urban atmosphere of Krakow, Poland, Isotopes in
960 Environmental and Health Studies, **40**(2): 129-143.
961
962 Zobitz, J. M., Burns, S.P., Reichstein, M., Bowling, D.R. (2008). Partitioning net ecosystem
963 carbon exchange and the carbon isotopic disequilibrium in a subalpine forest. Global Change
964 Biology, **14**(8): 1785-1800.
965
966 Zondervan, A., H. A. Meijer (1996). Isotopic characterisation of CO_2 sources during regional
967 pollution events using isotopic and radiocarbon analysis. Tellus B, **48**(4): 601-612.
968
969 Zhou, L., Conway, T.J., White, J.W., Mukai, H., Zhang, X., Wen, Y., Li, J. and MacClune, K.,
970 (2005). Long-term record of atmospheric CO_2 and stable isotopic ratios at Waliguan
971 Observatory: Background features and possible drivers, 1991–2002. Global Biogeochemical
972 Cycles, **19**(3): GB3021.
973

Figure 1. Dependence of the observed $\delta^{13}C$ on the H_2O mole fraction. The lines represent Equation 2. Error bars are ± one standard deviation of 1-min averages. The data in the left panel was obtained on October 1, 2014 using a 439 µmol mol^{-1} standard gas and the true $\delta^{13}C$ value of -32.8 ‰, and that in the right panel on June 10, 2015 using a 488 µmol mol^{-1} standard gas and the true $\delta^{13}C$ value of -34.1 ‰.

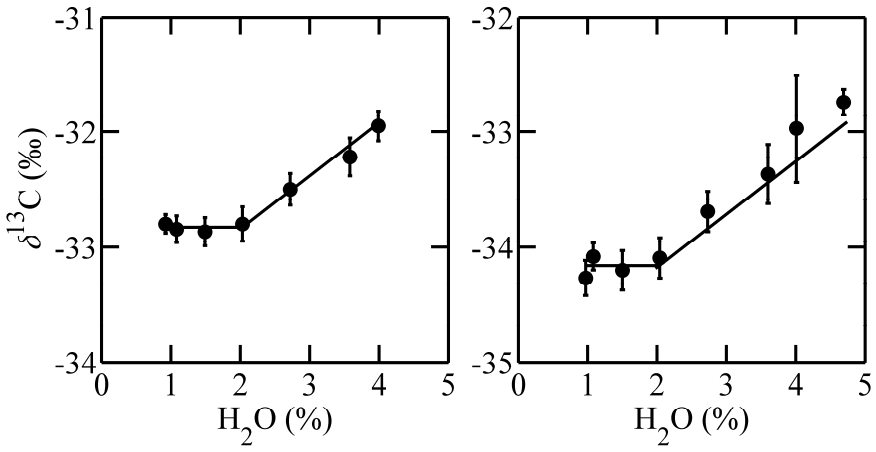

Figure 2. Monthly total CO_2 mole fraction (upper panel) and $\delta^{13}C$ (lower panel): Solid lines with circles: whole-day means; dashed lines with up triangles: daytime (10:00-16:00) means; dashed line with down triangles: nighttime (22:00-6:00) means; smooth solid lines, monthly means observed at WLG.

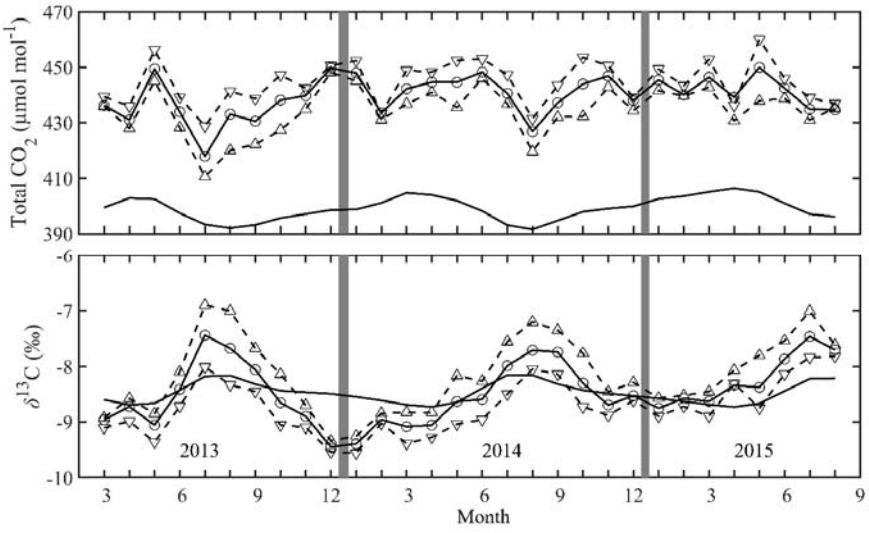

Figure 3. Mean diel variation of the CO_2 mole fraction (upper panels) and the $\delta^{13}C$ value (bottom panels) between March, 2013 and August, 2015.

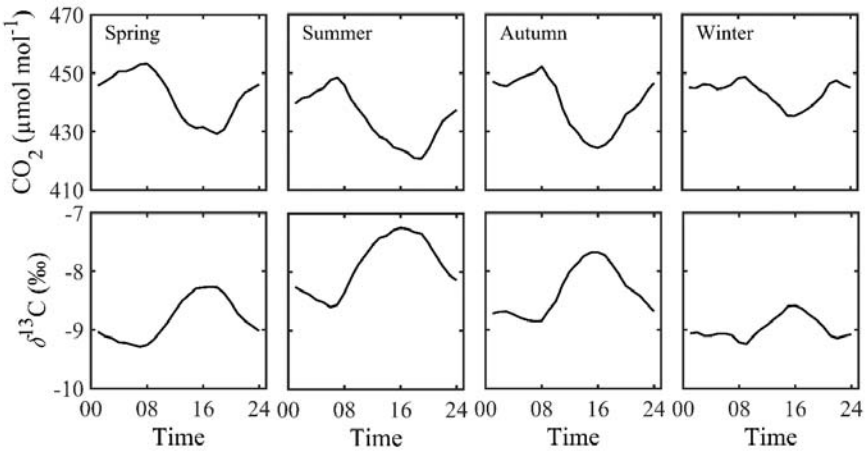

992 **Figure 4**. Application of the Miller-Tans method to the daytime (10:00-16:00) data obtained
993 in January 2014. Each data point is one hourly mean. The solid line is the least squares
994 regression according to Equation 3. Errors bounds on the regression coefficients are 95 %
995 confidence intervals.

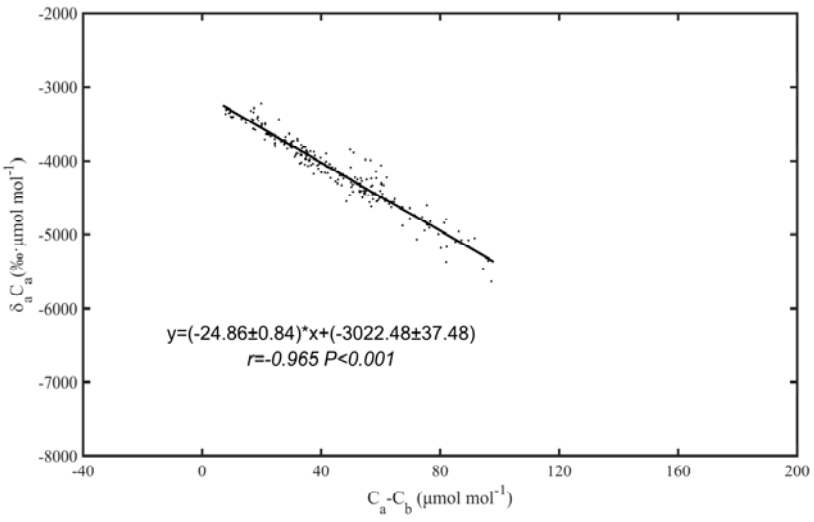

996

997 **Figure 5**. Same as Figure 4 but for nighttime (22:00-6:00) data obtained in January 2014.

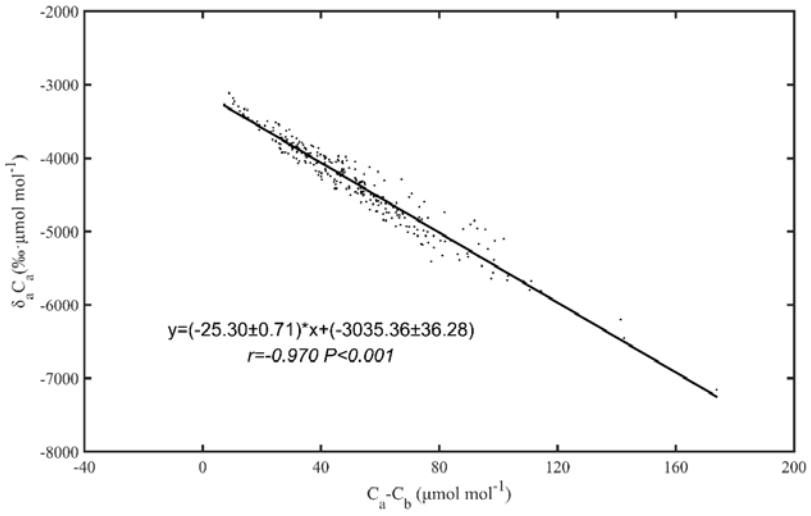

998

Figure 6. Time series of monthly $^{13}C/^{12}C$ ratio of surface sources in the YRD (a) and in Nanjing (b), obtained from daytime and nighttime measurement, respectively. The error bars are ± one standard deviation of the regression coefficient.

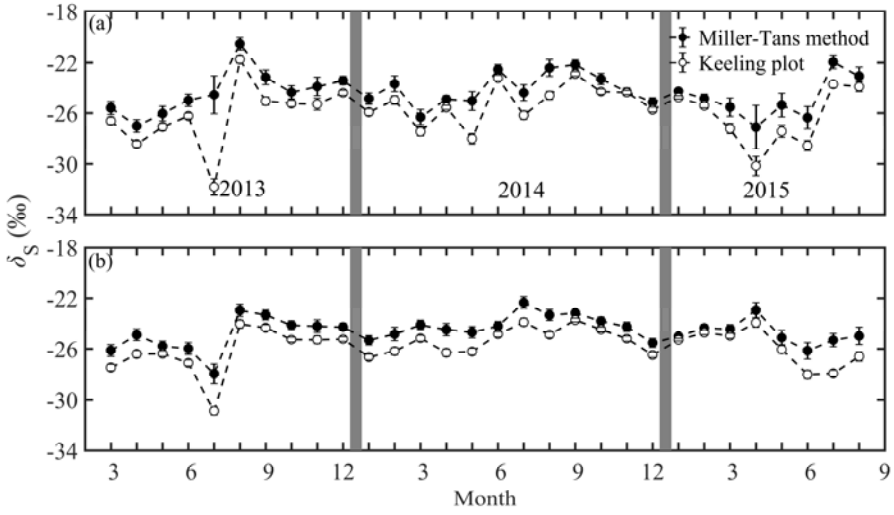

Figure 7. Time series of monthly net surface CO_2 flux (F_S), biological CO_2 flux (F_P), anthropogenic CO_2 flux excluding cement emission (F_F) and cement CO_2 flux (F_c) in the YRD. All the CO_2 mass fluxes are in mg m^{-2} s^{-1}. The flux terms F_F and F_c are assumed to have a 10 % uncertainty typical of fossil fuel consumption data. The partitioning results (F_P and F_S) are based on the source $^{13}C/^{12}C$ ratio derived from daytime atmospheric measurements.

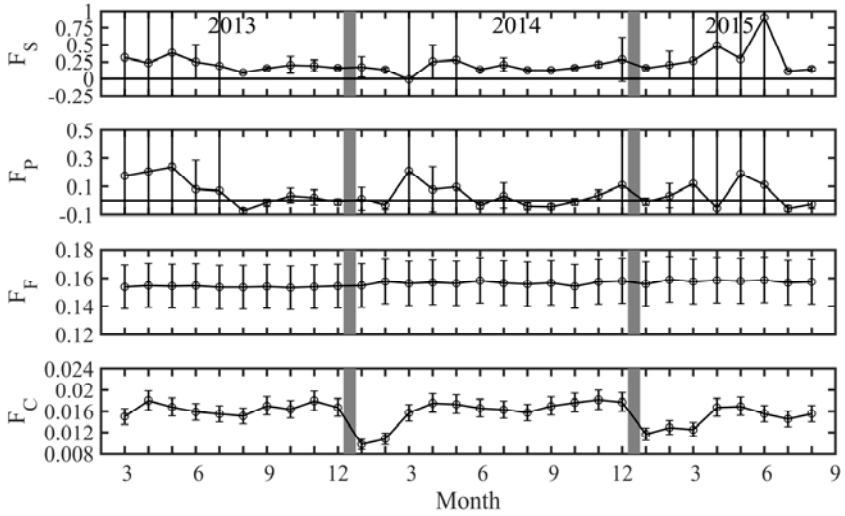

Figure 8. Time series of monthly net surface CO_2 flux (F_S), biological CO_2 flux (F_P), anthropogenic CO_2 flux excluding cement emission (F_F) and cement CO_2 flux (F_c) in Nanjing. All the CO_2 mass fluxes are in mg m^{-2} s^{-1}. The flux terms F_F and F_c are assumed to have a 10 % uncertainty typical of fossil fuel consumption data. The partitioning results (F_P and F_S) are based on the source $^{13}C/^{12}C$ ratio derived from nighttime atmospheric measurements.

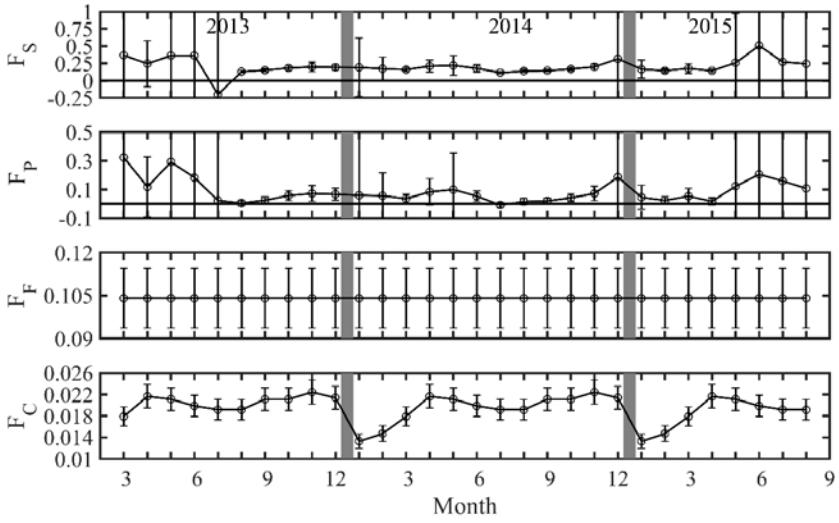

Table 1 Standard gases used for instrument calibration. The mean and standard deviation of the CO_2 mole fraction and $\delta^{13}C$ were based on 6 and 5 repeated measurements, respectively.

ID	CO_2 (μmol mol^{-1})	$\delta^{13}C$ (‰)	Period
1 Low	381.89 ± 0.99	-29.75 ± 0.27	Mar, 2013 - Aug, 2014
1 High	502.35 ± 0.28	-30.01 ± 0.18	Mar, 2013 - Aug, 2014
2 Low	380.92 ± 0.95	-29.75 ± 0.27	Sep, 2014 - Aug, 2015
2 High	501.05 ± 0.33	-30.01 ± 0.18	Sep, 2014 - Aug, 2015

1024 **Table 2** Percentage of "fossil-plus" sources and their $\delta^{13}C$ values for the YRD and Nanjing.

1025 The uncertainty in the total "fossil-plus" source is a weighted mean of the individual

1026 uncertainties.

	Percentage (%)		$\delta^{13}C$ (‰)		
Sources	YRD	Nanjing	YRD	Nanjing	References
Coal	70.0	52.3	-25.46 ± 0.39	-25.46 ± 0.39	Duan, 1995, Widory 2003
Gasoline	2.1	11.4	-28.69 ± 0.50	-28.69 ± 0.50	Widory and Javoy 2003
Diesel	3.2	1.6	-28.93 ± 0.26	-28.93 ± 0.26	Widory 2006
Fuel oil	2.1	0.3	-29.32 ± 0.15	-29.32 ± 0.15	Widory and Javoy 2003
Natural gas	2.7	5.0	-39.06 ± 1.07	-39.06 ± 1.07	Widory 2003
LPG	0.7	0.2	-31.70 ± 0.40	-31.70 ± 0.40	Widory 2006
Pig iron	8.7	12.7	-24.90 ± 0.40	-24.90 ± 0.40	Pan 2007
Crude steel	1.5	0.7	-25.28 ± 0.40	-25.28 ± 0.40	Wang 2013
Ammonia synthesis	9.0	15.9	-28.18 ± 0.55	-28.18 ± 0.55	An 2012
Total	100	100	-26.36 ± 0.42	-26.97 ± 0.46	

1027

1028 **Table 3**. Inventory data for the isotopic composition of surface CO_2 sources and their
1029 percentage of contribution in the YRD and in Nanjing. Here the "fossil-plus" category
1030 includes all non-cement anthropogenic emissions listed in Table 2. The cement isotopic ratio
1031 is based on Andres et al. (1994). The uncertain range in the biological isotope ratio is based
1032 on Vardag et al. (2016).

Sources	YRD		Nanjing	
	$\delta^{13}C$ (‰)	Percentage (%)	$\delta^{13}C$ (‰)	Percentage (%)
"Fossil-plus"	-26.36 ± 0.42	91.0	-26.97 ± 0.46	96.4
Cement	0 ± 0.30	9.0	0 ± 0.30	3.6
Anthropogenic	-23.99 ± 0.41	100	-26.00 ± 0.45	100
Biological	-28.20 ± 1.00	——	-28.20 ± 1.00	——

1033